

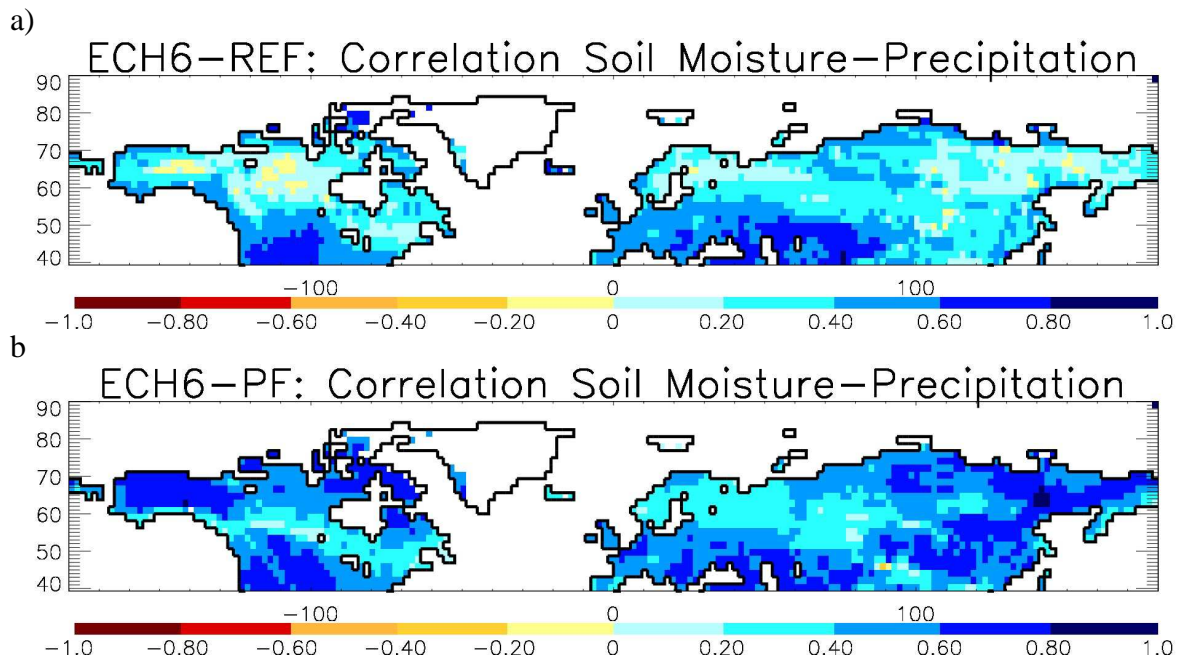
Reply to reviewers' comments

We thank Rene Orth and the anonymous reviewer for their thorough reading of the manuscript and their valuable remarks that helped us to improve the manuscript. In the following, the original reviewer comments are given in *italic* and all line numbers refer to the original submitted version that was reviewed if not mentioned otherwise. Note that after the removal of Fig. 1, the numbering of all figures has changed.

Reply to review of Rene Orth:

One main comment concerns the proposed soil moisture-precipitation feedback. While this feedback seems to be a plausible explanation of the reported results, more analysis is needed to confirm its operation. There may be many ways to do this, I could think of the following: Compute correlations between soil moisture and precipitation using seasonal values from all available years at any particular location. The resulting correlation maps for each simulation could be insightful.

Thank you for this suggestion. To add further analysis, we calculated the correlations between soil moisture and precipitation using monthly values from 1989-2009 for ECH6-REF and ECH6-PF. Then, we calculated the difference between correlation maps (ECH6-PF minus ECH6-REF). The resulting map (new Fig. 12c) shows that the correlation between soil moisture and precipitation is strongly increased in ECH6-PF over large parts of the northern high latitudes, especially over North America and eastern Siberia. This confirms the enabled soil moisture-precipitation feedback we identified over the northern high latitudes and for the area of the six largest Arctic catchments.



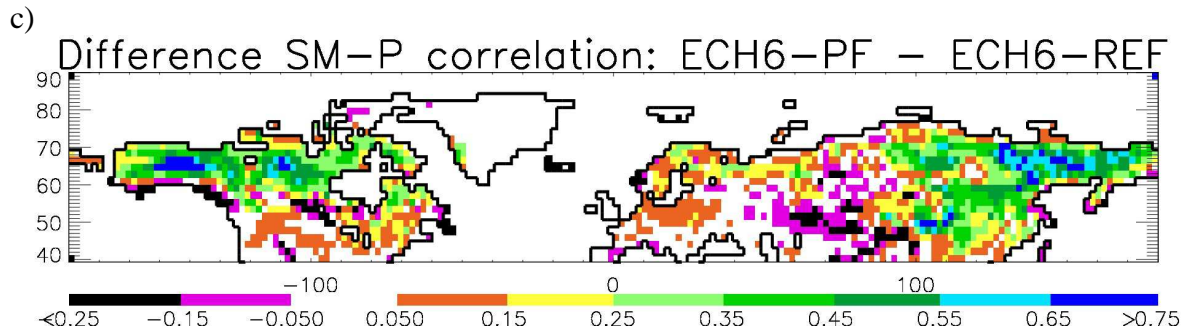


Fig. 12: Correlation of soil moisture and precipitation for a) ECH6-REF, b) ECH6-PF, and c) difference between ECH6-PF and ECH6-REF.

We added the figure and associated text in Sect. 4, starting in line 345:
 Our new finding of the importance of the positive soil moisture-precipitation feedback in northern high latitudes has been supported by correlations between soil moisture and precipitation using monthly values from 1989-2009. While there are higher correlations between soil moisture and precipitation in the mid-latitudes for ECH6-REF (Fig. 12a), the high latitudes are mostly characterized by rather low correlations using the reference version of JSBACH. Figure 12b and c show that the correlation between soil moisture and precipitation is strongly increased in ECH6-PF over large parts of the northern high latitudes, especially over North America and eastern Siberia. This confirms an increased coupling of soil moisture and precipitation, and, hence, also indicates that the soil moisture-precipitation feedback is highly enabled in these areas. This positive

Furthermore I am missing discussion and reasoning on the fact that the hydroclimatic changes following the introduction of the new PF scheme also occur in warmer regions (eg. aggravating the temperature bias in central youNorth America and southern Russia). Why is that? Why is it not possible to adapt the model modifications to prevent such effects? And in essence, is it more than a trade of model performance in one region against another region?

We added Fig. 13 and the following discussion in Sect. 4 as a new paragraph starting in line 351. Note that according to the comments of reviewer 1, we also added panels to the Figs. 2, 3, and 4 (now 1, 2 and 3) showing the changes in the respective variables between the two experiments:

Changes in hydrological cycle are mostly confined to areas where freezing and thawing of water play a role. To illustrate this, Fig. 13 shows the number of months where in the climatological average of 1989-2009, the upper soil layer is below 0°C in ECH6-PF. Changes in precipitation (Fig. 1) and surface solar irradiance (Fig. 3), indicating changes in cloud cover, are mostly located in regions where the upper layer is frozen for at least three months within the climatological average. Changes outside of regions with soil frost may be imposed by changed atmospheric humidity and heat transport from soil frost affected regions on the one hand. On the other hand, Ekici et al. (2014) also introduced a permanent, static organic top layer as part of the new JSBACH-PF soil scheme. If switched on, as in the current ECH6-PF simulation, it is considered globally uniform, thus introducing a soil isolating effect also outside permafrost regions. As a consequence, the partitioning of the surface heat balance is altered during snow-free months towards a decreased ground heat flux, which needs to be compensated for by the turbulent heat fluxes, in particular by the sensible heat flux. This in turn contributes to the warming of the 2m air temperature which can be seen also in areas

without any soil frost (Fig. 2). Even though the uniform organic insulation layer was implemented globally, Fig. 12 shows that the correlation between soil moisture and precipitation advances strongly in northern high latitudes only while this correlation has nearly not changed in the temperate zone and in particular in drought-dominated areas in south-east Europe or mid-west USA. Note that currently, the land surface scheme has been further advanced by a mechanistic model of mosses and lichens dynamics (Porada et al., 2016) which will replace the actual static organic top layer for soil insulation. This will enable a more realistic representation of the temporal and spatial variation of the soil insulation.

Added reference:

Porada, P., Ekici, A., and Beer, C.: Effects of bryophyte and lichen cover on permafrost soil temperature at large scale, *The Cryosphere Discuss.*, doi:10.5194/tc-2015-223, in review, 2016.

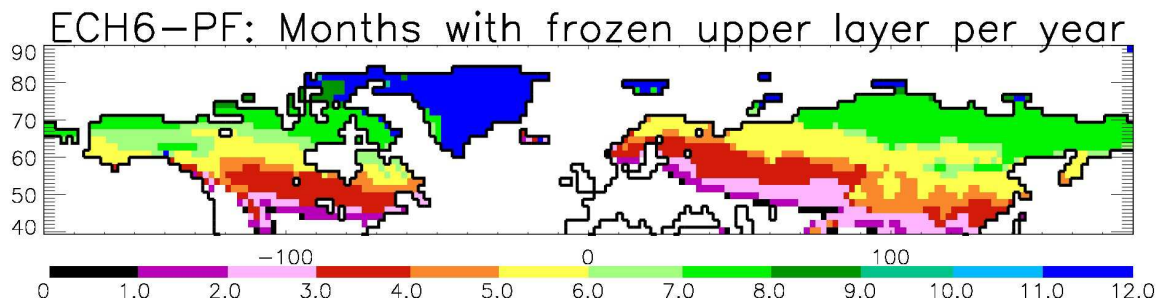


Fig. 13: Number of months where in the climatological average of 1989-2009, the upper soil layer is below 0°C in ECH6-PF.

Another general comment refers to the terminology used in the paper. The authors should state more clearly that they refer to liquid moisture if they use 'soil moisture'.

In end of Sect. 2.1, we added the following text:

“Note that in the following the term soil moisture generally refers to the liquid soil moisture if not mentioned otherwise. In this respect, total soil moisture refers to the sum of liquid and frozen soil moisture.”

In addition, we thoroughly checked the usage of the corresponding terms throughout the manuscript, and corrected them where it seems appropriate.

Furthermore Figures 6 and 10 present results already contained in Figures 2-4. I understand the motivation of the authors to first present a global picture and to then focus on particular regions. However, maybe the text describing these figures can be shortened to be less repetitive.

We shortened the text describing Figures 6 and 10 (now 5 and 9).

Lines 267-269 are modified as:

Consistent with Fig. 1, the large wet bias in the summer precipitation of ECH6-REF is strongly reduced in ECH6-PF (Fig. 5c). This ...

Lines 288-294 are modified as:

The decreased ET during warm months, however, brings about less evaporative cooling of the land surface and a reduced upward moisture flux into the atmosphere that in turn seems to

reduce cloud cover, and, hence SSI is increased in ECH6-PF (Fig. 9c, see also Fig. 3). Both of these effects result in a further increase of the summer warm bias in 2m air temperature (Fig. 9a, see also Fig. 2).

Specific comments

line 24: insert 'the' before MPI-ESM

Corrected as suggested.

line 45: please explain 'Pg of C'

Here, we updated the text by more recent results from line 41 onwards and also clarified the use of "Pg of C":

... high carbon contents (Ping et al., 2008, Nature Geoscience) leading to a total pan-Arctic estimate of 1300 Pg of soil carbon (C) in these areas (Hugelius et al., 2014, Biogeoscience), which is twice the amount of the atmosphere's content. Moreover, the high ...

line 57: CH4 does not simply 'become' CO2

We modified the text:

... after which it is converted to CO2 by oxidation.

line 82: replace ', which' with '. The parameterizations'

Corrected as suggested.

line 107: What is the 'potential rate'?

We modified the text:

...at the potential rate imposed by the atmospheric conditions, i.e. the potential evapotranspiration.

line 126: abbreviation ESM was introduced earlier

We modified the text:

... components of the ESM of the ...

lines 143/144: How can properties 'decrease'?

Soil hydraulic conductivity and diffusivity are hydraulic properties of the soil. They depend on soil moisture and, hence, may increase or decrease when soil moisture increases or decreases, respectively.

We modified the text:

... content may decrease when soil moisture freezes (such as, e.g., the hydraulic conductivity).

line 145: delete 'now'

Corrected as suggested.

line 146: confusing sentence, please rephrase

We modified the text:

In the original snow scheme, the snow is thermally growing down inside the soil, i.e. the snow cover becomes part of the soil temperature layers so that soil temperatures are mixed with snow temperatures. In the new scheme, snow is accumulated on top

line 154: replace 'for' with 'during'

Corrected as suggested.

lines 154/155: delete 'so that'

Corrected as suggested and a ',' was inserted instead.

line 156: if it is switched off anyway why do you mention it?

It is switched off in the default application of JSBACH3, but not in our study as setting this switch is hydrologically more sensible, and GPP is not of interest in the present study.

lines 178-180: Please clarify if you are using the WATCH or the WFDEI forcing data.

We are only using WFDEI. We modified the text:

... the recent global WATCH dataset of hydrological forcing data (WFDEI; ...

line 194-195: How do your results differ if you consider all ET datasets instead of only the diagnostic datasets?

We chose to compare our simulated ET only with the diagnostic estimates of ET, not with other model data. If considering the ET from all datasets, the ET over the six largest Arctic river catchments is rather similar to those from the diagnostic estimates, especially in the summer (Fig. R1).

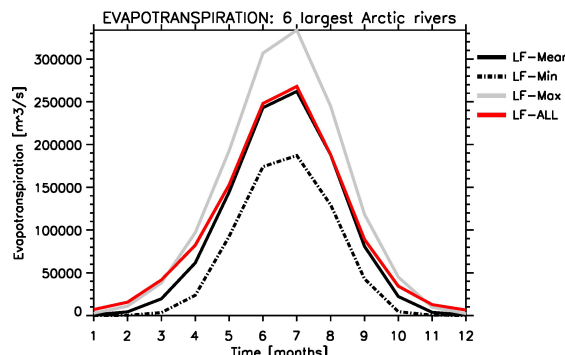


Fig. R1: Mean ET of all LF datasets compared the mean, minimum and maximum diagnostic estimates from the LandFlux Eval (LF) dataset.

line 217: why the fifth layer? and how deep is that?

As the upper layers usually thaws during the summer (the maximum thawing depth is called active layer depth), we chose the lowest layer of the JSBACH soil column, which is certainly below the active layer. Its depth is ranging from 4.13 m to 9.83 m.

We added the following text to the model description in Sect. 2.1, line 136:

These five layers correspond directly to the structure used for soil temperatures and they are defined with increasing thickness (0.065, 0.254, 0.913, 2.902, and 5.7 m) down to a lower boundary at almost 10 m depth.

line 222: insert 'to' before 'avoid'

Corrected as suggested.

line 228 and elsewhere: please use consistent simulation names (ECHPF/ ECH6-PF)

We have thoroughly checked (and corrected where necessary) the document for the usage of ECH6-REF and ECH6-PF, which we had intended to use throughout the paper.

lines 234/235: 'evaluated ... to the evaluation'?

We modified the text:

...latitudes analogously to how the evaluation of surface water and energy fluxes of the CMIP5 version of MPI-ESM was conducted by Hagemann et al. (2013b).

line 301/302: Problem with brackets

We modified the brackets:

[Note that a version of MODIS albedo data was used where low quality data over the very high northern latitudes were filtered out in the boreal winter due to too low available radiation (A. Löw, pers. comm., 2016). Due to these missing data over mainly snow covered areas, MODIS albedo averaged over the six largest Arctic rivers is biased low in the winter].

line 339: Please clarify that the spring soil moisture deficit from increased discharge extents into the summer thanks to the soil moisture memory (e.g. Koster and Suarez 2001, Orth and Seneviratne 2012)

We modified the text and added:

This spring soil moisture deficit from the increased discharge extents into the boreal summer due to the soil moisture memory (e.g. Koster and Suarez 2001, Orth and Seneviratne 2012), when it actually causes ...

We added the following references:

Koster, R. D., and Suarez, M. J.: Soil moisture memory in climate models. *J. Hydrometeorol.*, 2, 558-570, 2001.

Orth, R., and Seneviratne, S.I.: Analysis of soil moisture memory from observations in Europe. *J. Geophys. Res. - Atmospheres*, 117, D15115, 2012.

line 361/362: This is wrong, these studies compute diagnostics at seasonal time scales!

We agree with regard to Koster et al. (2004) as here we mixed something up. We disagree with regard to Teuling et al. (2009). For the results described in their Fig. 1, they explicitly note: "In Figure 1 we display the correlation of ET with incident solar (global) radiation (R_g), respectively precipitation (P), on the yearly timescale in the GSWP-2 reanalysis."

We modified the text, starting in line 361:

... (Seneviratne et al., 2010). But on the one hand it can be assumed that many models participating in those earlier studies did not include the freezing and thawing of soil water. Thus, our reference simulation ECH6-REF is in line with results reported in the literature, generally not showing a strong coupling between precipitation and soil moisture in permafrost regions, such as indicated by the rather low correlation values in Fig. 12a. Only the ECH6-PF simulation using advanced soil physics shows that such strong coupling indeed is present (Fig. 12b). On the other hand, only annual mean diagnostics were considered in some of those earlier studies (e.g. Teuling et al., 2009). In other land-atmosphere coupling studies, that, e.g., followed the GLACE protocol such as Koster et al. (2004), prescribed soil moisture conditions were used that were similar to the average soil moisture climatology. Here, it seems that the differences between the simulations with free and prescribed soil moisture in GLACE type simulations may be not large enough to reveal a large-scale feedback over the high latitudes. This may only be possible by an experimental design where more pronounced

summer soil moisture changes are introduced. Note that in the present study, these pronounced changes were introduced not due to an artificial design, but they were caused by the implementation of previously missing frozen soil physics into the model. Our study has shown that spring moisture deficits can lead to soil moisture conditions during the boreal summer that allow for an advanced land atmosphere coupling and a positive soil moisture-precipitation feedback over the northern high latitudes.

lines 388/389: replace 'not an issue' with 'beyond the scope of the present study'
Corrected as suggested.

Figure 1: It almost seems to me as if the new parameterization leads to too little permafrost extent.

If also areas with non-continuous permafrost are considered, we may agree with the reviewer. This would be consistent with the already existing (in ECH6-REF) and increased (in ECH6-PF) warm bias. But as mentioned in Sect. 2.5, those non-continuous areas cannot be simulated as the JSBACH land surface scheme does not include sub-grid heterogeneity for soil temperatures. We try to estimate part of the spatial heterogeneity by temporal discontinuities in the permafrost diagnostic (c.f. Sect. 2.5). But this seems to be insufficient to represent the spatial discontinuities in permafrost areas. Thus, we think that the fairest comparison of the simulated permafrost areas is with the observed continuous permafrost areas (dark blue colour) in Fig. 1a, where some improvement can be seen in ECH6-PF.

Note that due to a comment of reviewer 1 we were re-thinking about the value of the figure for the whole study and concluded that the figure itself is not directly related to the main feedback topic, and, thus, also not really helpful for the conclusions of the study. Consequently we removed the figure, the associated Sect. 2.5. and the associated first paragraph of Sect. 3.

Figures 1-4: please label the color bars

We are somewhat puzzled by this remark as the colour steps are already labelled, and variable and unit are provided in the figure captions except for Fig. 1 that we have now removed.

Figure 7: include dashed blue line in legend

Included as suggested. Consequently, we now use separate legends for panels a,b and c,d instead of one legend for all panels.

Figure 8: repetitive titles, no x-axis label

We removed the title above the figure panel, but the x-axis is already labelled with 'Time [months]'.

Figure 12: Your line of arguments is that first the soil freezes and then more runoff occurs such that consequently soil moisture is decreased. This is not clear from this scheme.

We have redrawn the scheme so that it starts now with the soil freezing on the left, and we have also somewhat simplified it (now it became Fig. 11):

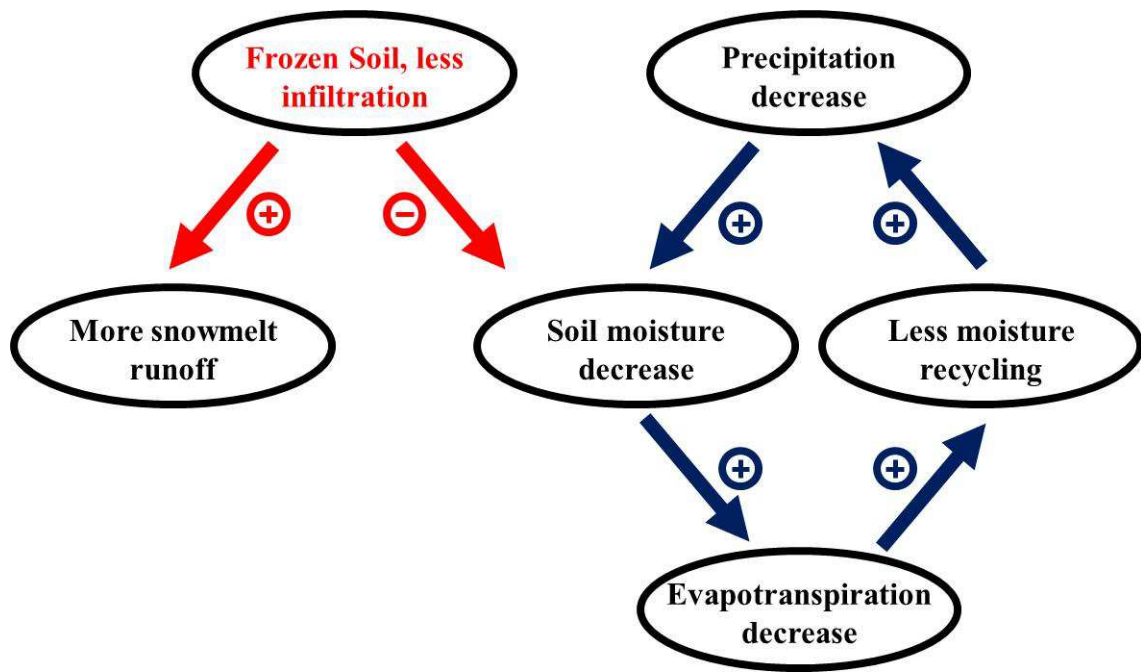


Fig. 11. Chain of processes involved in the soil moisture precipitation feedback over high latitudes. Red arrows indicate the initiation of the positive feedback loop by the presence of frozen soil, blue arrows indicate the loop itself.

Reply to anonymous reviewer 1:

We thank the reviewer for his/her thorough reading of the manuscript and the valuable remarks that helped us to improve the manuscript. Following our general reply, the original reviewer comments are given in *italic* and all line numbers refer to the original submitted version that was reviewed if not mentioned otherwise. Note that after the removal of Fig. 1, the numbering of all figures has changed.

General reply

According to the remarks of reviewer 1 we feel that our current text may have led to a partial misunderstanding. We do not propose that soil freezing and thawing processes lead to a *new* feedback, but that these processes enable a *known* feedback to become *active* over the northern high latitudes. In order to avoid a possible misunderstanding we modified the title, the abstract as well as the beginning and the end of the discussion section as follows:

New title:

Soil frost-enabled soil moisture precipitation feedback over northern high latitudes

Modified abstract: starting in line 13

... permafrost. The currently observed global warming is most pronounced in the Arctic region and is projected to persist during the coming decades due to anthropogenic CO₂ input. This warming will certainly have effects on the ecosystems of the vast permafrost areas of the high northern latitudes. The quantification of such effects, however, is still an open question. This is partly due to the complexity of the system, including several feedback mechanisms between land and atmosphere. In this study we contribute to increasing our understanding of such land-atmosphere interactions using an Earth system model (ESM) which includes a representation of cold region physical soil processes, especially the effects of freezing and thawing of soil water on thermal and hydrological states and processes. The coupled atmosphere-land models of the ESM of the Max Planck Institute for Meteorology, MPI-ESM, have been driven ...

and line 28:

... subsequent reduction of soil moisture enables a positive feedback ...

Added and modified text in line 116-117:

Only Takata and Kimoto (2000) conducted a kind of precursor to our study who used a very coarse resolution atmospheric GCM (600 km resolution), but they neither used large-scale observations to evaluate the results of their study nor specifically addressed land-atmosphere feedbacks. Thus, soil moisture feedbacks to the atmosphere related to cold region soil processes have generally been neglected so far.

Added reference:

Takata, K., and Kimoto, M.: A numerical study on the impact of soil freezing on the continental-scale seasonal cycle, J. Meteor. Soc. Japan, 78, 199-221, 2000.

Modified discussion section, starting in line 330:

The results described in the previous section show that soil freezing and thawing processes enable the positive soil moisture-precipitation feedback (e.g. Dirmeyer et al., 2006;

Seneviratne et al., 2010) over large parts of northern mid- and high latitudes during the boreal summer. The chain of processes leading to and influencing this feedback ...

Modified discussion section in line 352:

... so far, even though in their coarse resolution GCM study, Takata and Kimoto (2000) found similar impacts to those shown in Fig. 11 induced by soil water freezing. Previously, the northern high latitudes have generally ...

Modified discussion section, starting in line 409:

We have shown that soil physical processes such as thawing and freezing have an impact on the regional climate over the high latitude permafrost areas. Flato et al. (2013) reported that CMIP5 GCMs tend to overestimate precipitation over northern high latitudes except for Europe and western Siberia. As many of these GCMs are still missing basic cold region processes, a missing interaction between soil moisture and precipitation in those GCMs is likely to contribute to this wet bias. An adequate implementation of physical soil processes into an ESM is only the first necessary step to yield an adequate representation of land-atmosphere interactions over the high latitudes. This also includes the incorporation of wetland dynamics, which will be the next step in the JSBACH development with regard to high latitudes, thereby following an approach of Stacke and Hagemann (2012). In addition, a reliable hydrological scheme for permafrost regions will allow investigations of related climate-carbon cycle feedback mechanisms (McGuire et al., 2006; Beer, 2008; Heimann and Reichstein, 2008).

Added references:

- Beer, C.: Soil science: The Arctic carbon count. *Nature Geoscience*, 1, 569-570, doi:10.1038/ngeo292, 2008.
- Heimann, M., and Reichstein, M.: Terrestrial ecosystem carbon dynamics and climate feedbacks, *Nature*, 451, 289-292, 2008.
- McGuire, A.D., Chapin III, F.S., Walsh, J.E. and Wirth, C.: Integrated regional changes in arctic climate feedbacks: Implications for the global climate system, *Annu. Rev. Environ. Resour.* 31, 61–91, doi:10.1146/annurev.energy.31.020105.100253, 2006.

Specific reply

Although the set-up of the experiment and the discussion of the results are well done and straightforward, I find some of the conclusions somewhat speculative. First, the existence of this positive feedback cannot be diagnosed very well from comparing two (ensemble) simulations of different model configuration. An experimental design is required in which this feedback loop is explicitly affected, which is not the case here.

We can fully understand the point by the reviewer here after reading the first version of the manuscript again. As we stated already above, there was a strong misunderstanding of our conclusions due to a lack of clarity in the text. If the conclusion was an identification of a new feedback mechanism then certainly specific artificial experiments representing different interactions between state variables would have been required. However, the soil moisture-precipitation feedback is well studied, e.g. in dry regions (e.g. Seneviratne et al. 2006, 2010; Seneviratne and Stöckli 2008; Dirmeyer et al. 2006; Koster et al. 2004). The major point of our investigation was that previously this feedback mechanism has not been considered in ESMs at high latitudes just because soil freezing and thawing processes were usually not represented. In this paper we show that these processes have a huge impact on soil state measures and with that also on atmospheric state measures and processes due to the soil

moisture-precipitation feedback. This has been demonstrated by model experiments with/without representing soil freezing and thawing.

In order to express the interactions between soil moisture content and precipitation more quantitatively, we have followed the advice of the other reviewer (Rene Orth) and present correlations of soil moisture and precipitation in the revised version of the manuscript. Consequently, we calculated the correlations between soil moisture and precipitation using monthly values from 1989-2009 for both, the control run ECH6-REF and the version including freezing and thawing, ECH6-PF. Then, we calculated the difference between correlation maps (ECH6-PF minus ECH6-REF). The resulting map (new Fig. 12c) shows that the correlation between soil moisture and precipitation is strongly increased in ECH6-PF over large parts of the northern high latitudes, especially over North America and eastern Siberia. This confirms an increased coupling of soil moisture and precipitation, and, hence, also indicates that the soil moisture-precipitation feedback is highly enabled over the northern high latitudes and for the area of the six largest Arctic catchments.

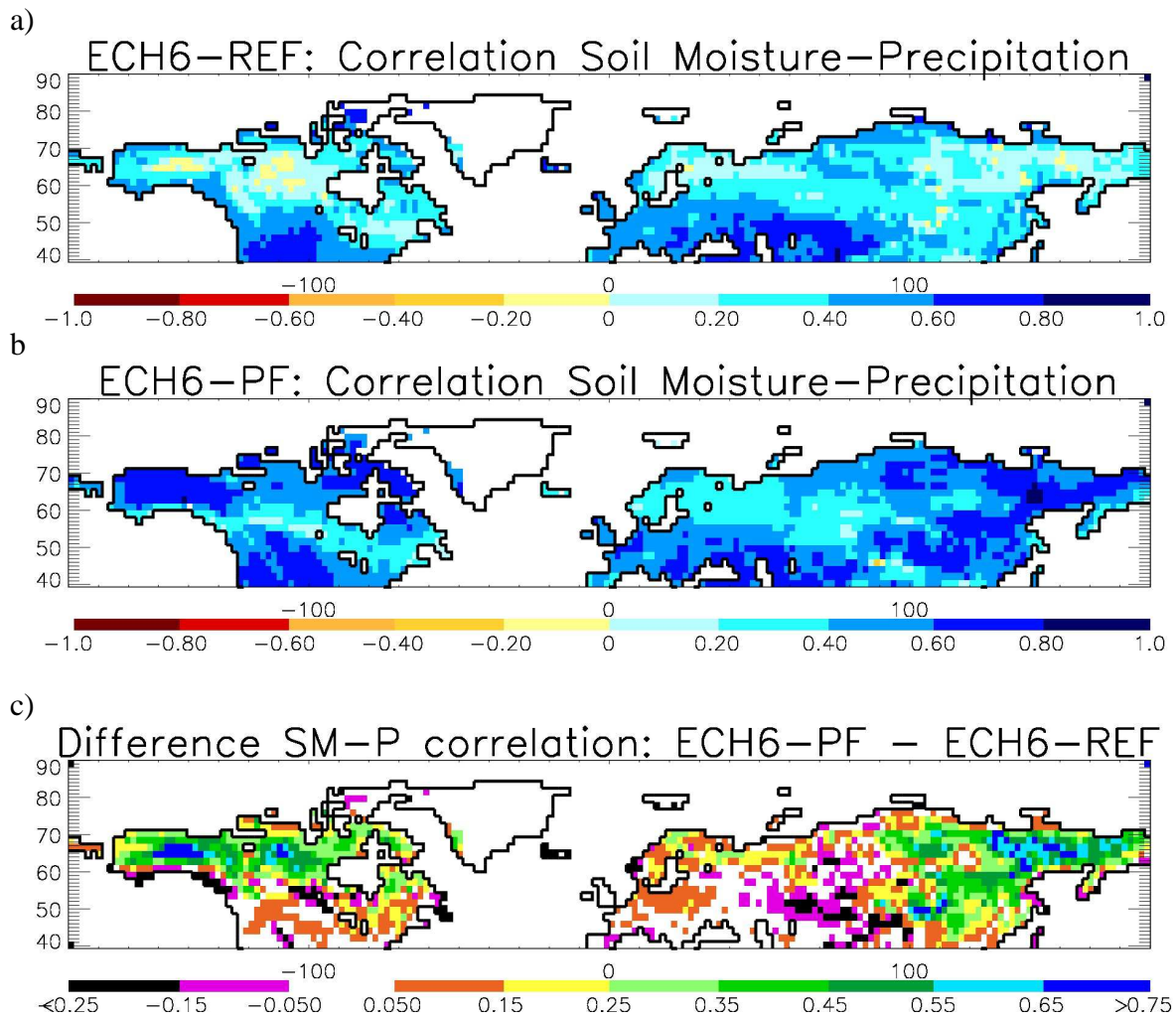


Fig. 12: Correlation of soil moisture and precipitation for a) ECH6-REF, b) ECH6-PF, and c) difference between ECH6-PF and ECH6-REF.

We added the figure and associated text in Sect. 4, starting in line 345:

Our new finding of the importance of the positive soil moisture-precipitation feedback in northern high latitudes has been supported by correlations between soil moisture and

precipitation using monthly values from 1989-2009. While there are higher correlations between soil moisture and precipitation in the mid-latitudes for ECH6-REF (Fig. 12a), the high latitudes are mostly characterized by rather low correlations using the reference version of JSBACH. Figure 12b and c show that the correlation between soil moisture and precipitation is strongly increased in ECH6-PF over large parts of the northern high latitudes, especially over North America and eastern Siberia. This confirms an increased coupling of soil moisture and precipitation, and, hence, also indicates that the soil moisture-precipitation feedback is highly enabled in these areas. This positive

It is surprising that earlier feedback studies as the ones by Koster et al and a few successors did not pick up this positive feedback in this area, in spite of targeting the same summer season as discussed extensively by the authors.

In order to add more discussion to this issue, we modified the text, starting in line 361:
... (Seneviratne et al., 2010). But on the one hand it can be assumed that many models participating in those earlier studies did not include the freezing and thawing of soil water. Thus, our reference simulation ECH6-REF is in line with results reported in the literature, generally not showing a strong coupling between precipitation and soil moisture in permafrost regions, such as indicated by the rather low correlation values in Fig. 12a. Only the ECH6-PF simulation using advanced soil physics shows that such strong coupling indeed is present (Fig. 12b). On the other hand, only annual mean diagnostics were considered in some of those earlier studies (e.g. Teuling et al., 2009). In other land-atmosphere coupling studies, that, e.g., followed the GLACE protocol such as Koster et al. (2004), prescribed soil moisture conditions were used that were similar to the average soil moisture climatology. Here, it seems that the differences between the simulations with free and prescribed soil moisture in GLACE type simulations may be not large enough to reveal a large-scale feedback over the high latitudes. This may only be possible by an experimental design where more pronounced summer soil moisture changes are introduced. Note that in the present study, these pronounced changes were introduced not due to an artificial design, but they were caused by the implementation of previously missing frozen soil physics into the model. Our study has shown that spring moisture deficits can lead to soil moisture conditions during the boreal summer that allow for an advanced land atmosphere coupling and a positive soil moisture-precipitation feedback over the northern high latitudes.

Also, such a positive feedback, when present, does require a sufficient amount of energy to generate a reasonable hydrological cycle. It should be shown that a significant fraction of available energy is not used for precipitation, by computing a kind of Budyko index.

Here, we are not 100 % sure if we correctly understand the reviewer's comment. The coupled atmosphere-land surface component of MPI-ESM used here is based on differential equations representing physical first principles and comprises closed energy and water budgets. Thus, no energy and water are lost or generated within the system. Consequently, both model versions are fully consistent with respect to the closed budgets. This means that there must be sufficient energy available to generate the simulated hydrological cycle, which also looks reasonable in ECH6-PF (e.g. Fig. 6 (now 5) a, c, Fig. 7a (now 6a)).

We calculated the Budyko index following Arora (2002, The use of the aridity index to assess climate change effect on annual runoff, J. Hydrology 265: 164-177) as the available energy R_{net} (annual mean net radiation at the surface) divided by precipitation P and the latent heat of vaporization L for both experiment. The corresponding maps (Fig. R2) show that for ECH6-

PF, the high latitudes generally get somewhat more arid than for ECH6-REF. This is consistent with the identified feedback loop where the reduced soil moisture leads to reduced summer precipitation. We do not think that this provides much additional information so we would not include this figure in the manuscript.

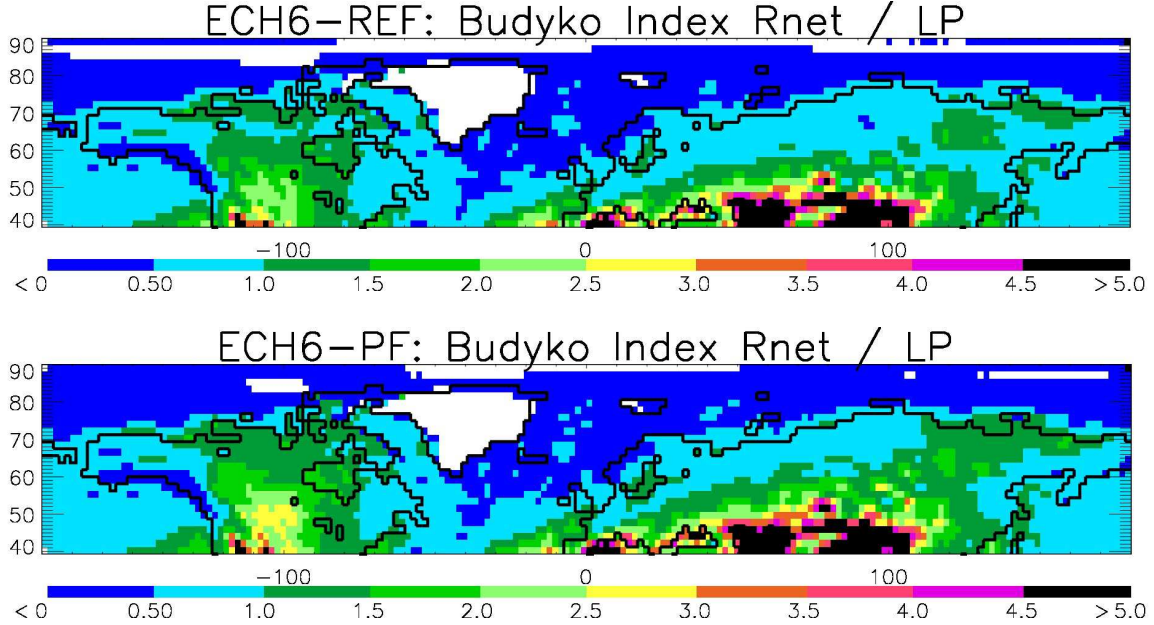


Fig. R2: Budyko dryness index for ECH6-REF (upper panel) and ECH6-PF (lower panel) derived from annual mean net surface radiation and precipitation.

Second, it is somewhat unclear why the large effects of the new scheme also tend to extend to areas where snow and permafrost occurrence is much less pronounced. Apparently strong alterations of the scheme to the entire soil hydrological balance are imposed.

We add the following discussion and the new Fig. 13 in Sect. 4 as a new paragraph starting in line 351. Note that according to the reviewer's comment listed below, we also added panels to the Figs. 2, 3, and 4 (now 1, 2, and 3) showing the changes in the respective variables between the two experiments:

Changes in the hydrological cycle are mostly confined to areas where freezing and thawing of water play a role. To illustrate this, Fig. 13 shows the number of months where in the climatological average of 1989-2009, the upper soil layer is below 0°C in ECH6-PF. Changes in precipitation (Fig. 1) and surface solar irradiance (Fig. 3), indicating changes in cloud cover, are mostly located in regions where the upper layer is frozen for at least three months within the climatological average. Changes outside of regions with soil frost may be imposed by changed atmospheric humidity and heat transport from soil frost affected regions on the one hand. On the other hand, Ekici et al. (2014) also introduced a permanent, static organic top layer as part of the new JSBACH-PF soil scheme. If switched on, as in the current ECH6-PF simulation, it is considered globally uniform, thus introducing a soil isolating effect also outside permafrost regions. As a consequence, the partitioning of the surface heat balance is altered during snow-free months towards a decreased ground heat flux, which needs to be compensated for by the turbulent heat fluxes, in particular by the sensible heat flux. This in turn contributes to the warming of the 2m air temperature which can be seen also in areas without any soil frost (Fig. 2). Even though the uniform organic insulation layer was implemented globally, Fig. 12 shows that the correlation between soil moisture and precipitation advances strongly in northern high latitudes only while this correlation has

nearly not changed in the temperate zone and in particular in drought-dominated areas in south-east Europe or mid-west USA. Note that currently, the land surface scheme has been further advanced by a mechanistic model of mosses and lichens dynamics (Porada et al., 2016) which will replace the actual static organic top layer for soil insulation. This will enable a more realistic representation of the temporal and spatial variation of the soil insulation.

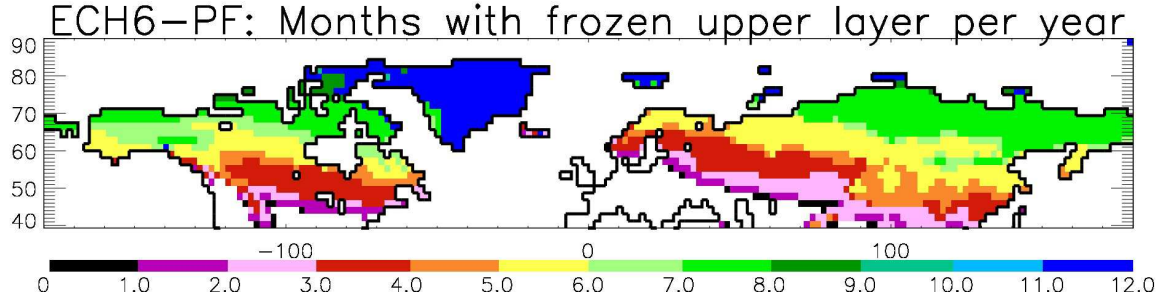


Fig. 13: Number of months where in the climatological average of 1989-2009, the upper soil layer is below 0°C in ECH6-PF.

For both notions a different presentation of results would be favorable. Particularly figs 2-4 should be presented as a difference between the 2 model versions rather than (or in addition to) the difference to observations. This provides a better connection to fig 12, and allows a discussion on the spatial structure of the supposed feedback.

As suggested, we added a third panel to each of the figs. 2-4 (now 1-3) that shows the respective differences between the two experiments. These difference maps are shown in the following as the new figures 1c, 2c and 3c.

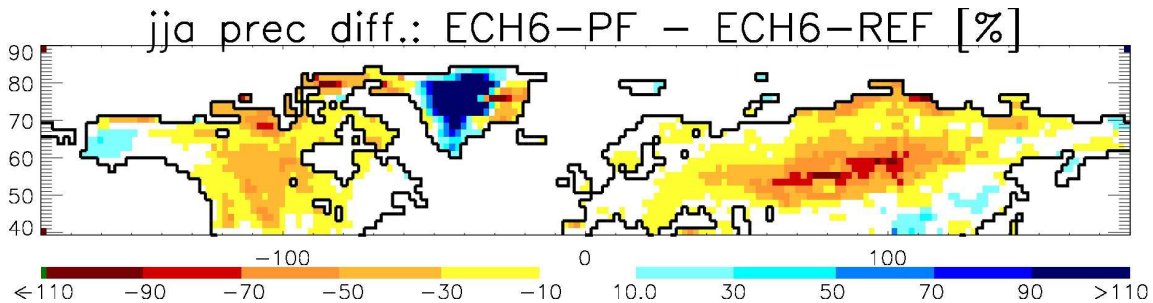


Fig. 1c: Precipitation difference between ECH6-PF and ECH6-REF [in % of WFDEI precipitation].

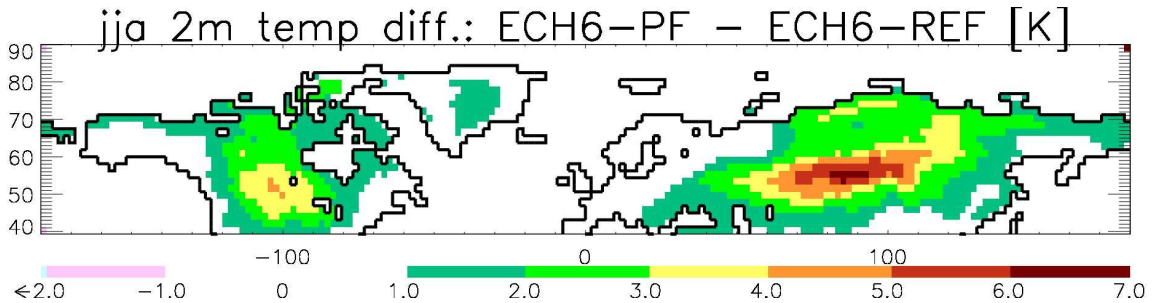


Fig. 2c: 2m temperature difference between ECH6-PF and ECH6-REF.

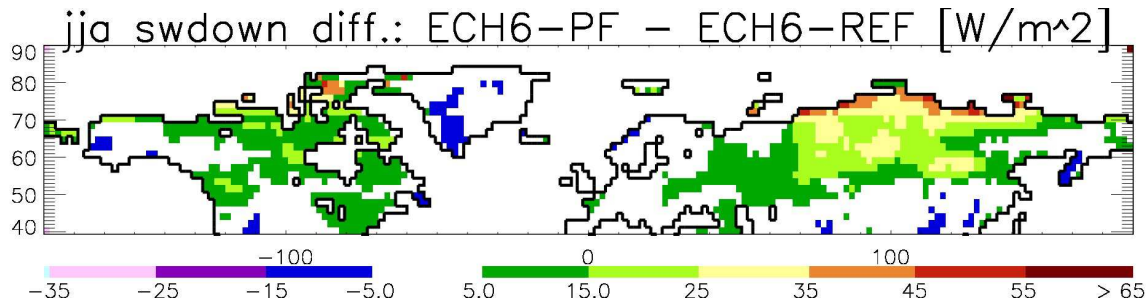


Fig. 3c: Surface solar incoming radiation difference between ECH6-PF and ECH6-REF.

Specific comments

L57: “becomes CO₂” sounds a bit odd

We modified the text:

... after which it is converted to CO₂ by oxidation.

L76: *whereat* -> *whereas*

Corrected as suggested.

L108: *excluded from*

Corrected as suggested.

Fig 1: the difference in permafrost area is not very clear nor impressive

On the one hand, a validation of the simulated permafrost area is not the focus of the present study as this has been done by Ekici et al. (2014). They forced the JSBACH land surface scheme offline with prescribed quasi-observed forcing and showed that winter temperatures were underestimated if only liquid water exists in the model, i.e. if no thawing/freezing is considered. On the other hand, we think that it is indeed rather good that there is no large difference, as it implies that no really huge differences have been imposed to the simulated climatological energetic mean state of the soil through the use of the new PF scheme. In other words, the use of physical cold region soil processes does not necessarily imply a completely different permafrost distribution. Note that the permafrost map is generated through diagnosing permafrost purely from a soil temperature criterion. Thus, already the soil temperatures in ECH6-REF yield a reasonable permafrost distribution.

If also areas with non-continuous permafrost are considered, an underestimation of permafrost areas might be indicated, which would be consistent with the already existing (in ECH6-REF) and increased (in ECH6-PF) warm bias. But as mentioned in Sect. 2.5, those non-continuous areas cannot be simulated as the JSBACH land surface scheme does not include sub-grid heterogeneity for soil temperatures. We try to estimate part of the spatial heterogeneity by temporal discontinuities in the permafrost diagnostic (c.f. Sect. 2.5). But this seems to be insufficient to represent the spatial discontinuities in permafrost areas. Thus, we think that the fairest comparison of the simulated permafrost areas is with the observed continuous permafrost areas (dark blue colour) in Fig. 1a, where some improvement can be seen in ECH6-PF.

But thanks to your comment we were re-thinking about the value of the figure for the whole study and concluded that the figure itself is not directly related to the main feedback topic, and, thus, also not really helpful for the conclusions of the study. Consequently we removed the figure, the associated Sect. 2.5. and the associated first paragraph of Sect. 3.

L362: Koster et al 2004 did not present annual means but JJA means

Yes, we agree. Here, we mixed something up and have modified the text (see also response to your second major comment).

L406: the advection of warm air is also of influence on the recycling ratio that is computed.

You should address this aspect

We modified the text in lines 405-406:

Further contributions to this warm bias might be related to a too weak vertical mixing of heat within the boundary layer or too much advection of warm air. The latter may also influence the recycling ratio of water within and outside regions of soil frost.

Fig 6: the dark blue and black colors are too similar to be distinguishable

We modified the dark blue line in all respective figures by making it brighter.

Fig 8: which model is shown here? Why only one model?

We only show results for ECH6-PF, since ECH6-REF does not include any freezing, and, hence no frozen soil moisture. We added the following text:

...soil moisture (1989-2009) in ECH6-PF over the curve). Note that for ECH6-REF, this is zero as no freezing is regarded.

Fig 12: what is the role of temperature in this diagram? It seems an important variable

We agree that temperature plays a role for freezing and thawing of soil moisture. But for this hydrological feedback loop that is initiated by the introduction of frozen soil, temperature does not play a first order active role. Its secondary effect is a general warming (less cooling of the surface due to the reduced evapotranspiration, more heating of the surface to the increased incoming solar radiation induced by the lower cloud cover – see also, e.g., lines 288-294).

In order to mention its general importance for soil freezing and thawing processes, we added the following in line 350:

Since air temperature is a main driver of soil freezing and thawing processes, there are more indirect interactions between energy and water balances which call for even more advanced factorial model experiments in the future.

Reply to editor's remark:

We thank the editor Christoph Heinze for his work and his additional remark.

In view of the audience of Earth System Dynamics you may elaborate a bit more on the general implications of your findings for research in other relevant disciplines.

In addition to modifications of the last paragraph in Sect. 4 in response to the remarks of reviewer 1, we added another paragraph in the end of the section:

Our findings demonstrate that soil freezing and thawing induce a much stronger coupling of land and atmosphere in northern high latitudes than previously thought. The additional importance of the positive soil moisture precipitation feedback in high latitudes will have a strong impact on future climate projections in addition to other biophysical (e.g. albedo) or biogeochemical (e.g. climate-carbon cycle) feedback mechanisms. Therefore, the findings of this study additionally highlight the importance of permafrost ecosystem functions in relation to climate.

Please note that we also updated a statement in the introduction (lines 41-46) with more recent literature:

... contents (Ping et al., 2008) leading to a total pan-Arctic estimate of 1300 Pg of soil carbon (C) in these areas (Hugelius et al., 2014), which is twice the amount of the atmosphere's content. Moreover, the ...

Soil frost-~~induced~~enabled soil moisture precipitation feedback over ~~high~~-northern high latitudes

Stefan Hagemann^{1*}, Tanja Blome¹, Altug Ekici² and Christian Beer³

¹ Max-Planck-Institut für Meteorologie, Bundesstr. 53, 20146 Hamburg, Deutschland,
* Tel.: +49 40 4117 3101, Email: stefan.hagemann@mpimet.mpg.de

² Earth System Sciences, Laver Building, University of Exeter, Exeter, UK

³ Department of Environmental Science and Analytical Chemistry (ACES) and Bolin Centre for Climate Research, Stockholm University, Stockholm, Sweden.

11 **Abstract**

12 Permafrost or perennially frozen ground is an important part of the terrestrial cryosphere;
13 roughly one quarter of Earth's land surface is underlain by permafrost. The ~~impact of the~~
14 currently observed global warming ~~is most pronounced in the Arctic region and, which~~ is
15 projected to persist during the coming decades due to anthropogenic CO₂ input. ~~This~~
16 warming will certainly ~~hasve~~ effects ~~foron~~ the ecosystems of the vast permafrost areas of the
17 high northern latitudes. The quantification of ~~these such~~ effects, however, is ~~scientifically~~ still
18 an open question. This is partly due to the complexity of the system, ~~whereincluding~~ several
19 feedback ~~mechanisms s are interacting~~ between land and atmosphere, ~~sometimes~~
20 ~~counterbalancing each other. In this study we contribute to increasing our understanding of~~
21 ~~such land-atmosphere interactions using an~~ ~~Moreover, until recently, many global circulation~~
22 ~~models (GCMs) and~~ Earth system models (ESMs) ~~lacked the sufficient~~~~which includes a~~
23 representation of cold region physical soil processes ~~in their land surface schemes~~, especially
24 ~~of~~ the effects of freezing and thawing of soil water ~~for on thermal and hydrological states and~~
25 ~~processes both energy and water cycles. Therefore, it will be analysed in the present study how~~
26 ~~these processes impact large scale hydrology and climate over northern hemisphere high~~
27 ~~latitude land areas. For this analysis, t~~ ~~The coupled atmosphere-land models part of the ESM~~
28 ~~of the Max Planck Institute for Meteorology, MPI-ESM, ECHAM6 JSBACH, is hasve been~~
29 driven by prescribed observed SST and sea ice in an AMIP2-type setup with and without
30 newly implemented cold region soil processes. Results show a large improvement in the
31 simulated discharge. On one hand this is related to an improved snowmelt peak of runoff due
32 to frozen soil in spring. On the other hand a subsequent reduction of soil moisture ~~leads~~
33 ~~enables to~~ a positive ~~land atmosphere~~ feedback to precipitation over the high latitudes, which
34 reduces the model's wet biases in precipitation and evapotranspiration during the summer.
35 This is noteworthy as soil moisture – atmosphere feedbacks have previously not been in the

36 research focus over the high latitudes. These results point out the importance of high latitude
37 physical processes at the land surface for the regional climate.

38 **Keywords:** Soil moisture – precipitation feedback, soil water freezing, permafrost regions,
39 global climate modelling, high latitudes

40 **1 Introduction**

41 Roughly one quarter of the northern hemisphere terrestrial land surface is underlain by
42 permafrost (Brown et al., 1997; French, 1990), which is defined as ground that is at or below
43 zero degrees Celsius for more than two consecutive years. Permafrost soils build a globally
44 relevant carbon reservoir as they store large amounts of deep-frozen organic material with
45 high carbon contents ([Ping et al., 2008](#)) leading to a total pan-Arctic estimate of 1300 Pg of
46 soil carbon (C) in these areas ([Hugelius et al., 2014](#)). ~~In recent years, estimates for the amount~~
47 ~~of carbon stored in soils have attracted more and more attention, and here especially the~~
48 ~~consideration of the vast permafrost regions increased numbers of these estimates drastically~~
49 ~~(Tarnocai et al., 2009; Zimov et al., 2006; Schuur et al., 2008; McGuire et al., 2009). It is~~
50 ~~believed to store between 1400 and 1800 Pg of C in the upper few meters of the soil (Schuur~~
51 ~~et al., 2008), which would be, which is~~ twice the amount of the atmosphere's content.
52 Moreover, The high northern latitudes are one of the critical regions of anthropogenic climate
53 change, where the observed warming is clearly above average due to the so-called Arctic
54 Amplification (Solomon et al., 2007; ACIA, 2005). Climate model simulations project this
55 trend to continue (Serreze and Barry, 2011). The combination of the high C stocks in sub-
56 arctic and arctic soils with the pronounced warming in the affected regions could thus lead to
57 a positive [biogeochemical](#) feedback through the release of formerly trapped, 'deep-frozen' C
58 into the atmosphere, when near-surface permafrost thaws. For the thawed soils and their

59 biogeochemistry, it is decisive whether dry or wet conditions predominate: Aerobic
60 decomposition is relatively fast and leads to the release of CO₂, while anaerobic
61 decomposition is much slower and leads to the release of CH₄ as the main product of the
62 combustion of organic soil material. CH₄ is a much more potent greenhouse gas, but has a
63 shorter lifetime of about 10 years after which it is converted to becomes CO₂ by oxidation.
64 Therefore, not only the soil's temperature, but also its moisture status are important for the
65 assessment of the biogeochemical response to climatic conditions, and thus should be
66 represented in climate or Earth System models in a realistic and process-based manner. Thus,
67 the adequate representation of permafrost hydrology is a necessary and challenging task in
68 climate Earth system modelling.

69 Hagemann et al. (2013a) described relevant hydrological processes that occur in permafrost
70 areas and that should preferably be represented in models simulating interactions of
71 permafrost hydrology with vegetation, climate and the carbon cycle. The current state of the
72 representation of processes in general circulation models (GCMs) or Earth system models
73 (ESMs) can be obtained by systematic model intercomparison through the various climate
74 model intercomparison projects (CMIPs; Meehl et al., 2000) that have a long history within
75 the climate modelling community. Results from CMIPs provide a good overview on the
76 respective state of ESM model accuracy and performance. Koven et al. (2012) analysed the
77 performance of ESMs from the most recent CMIP5 exercise over permafrost areas. They
78 found that the CMIP5 models have a wide range of behaviours under the current climate, with
79 many failing to agree with fundamental aspects of the observed soil thermal regime at high
80 latitudes. This large variety of results originates from a substantial range in the level of
81 complexity and advancement of permafrost-related processes implemented in the CMIP5
82 models (see, e.g., Hagemann et al., 2013a), whereat whereas most of these models do not
83 include permafrost specific processes, not even the most basic process of freezing and melting

84 | thawing of soil water. Due to missing processes and related deficiencies of their land surface
85 | schemes, climate models often show substantial biases in hydrological variables over high
86 | northern latitudes (Luo et al., 2003; Swenson et al., 2012). Moreover, the land surface
87 | parameterizations used in GCMs usually do not adequately resolve the soil conditions (Walsh
88 | et al., 2005). The parameterizations, which often rely on either point measurements or on
89 | information derived from satellite data. Therefore, large efforts are ongoing to extend ESMs
90 | in this respect, in order to improve simulated soil moisture profiles and associated ice
91 | contents, river discharge, surface and sub-surface runoff. The ESM improvement over
92 | permafrost areas was, e.g., one of the research objectives of the European Union Project
93 | PAGE21 (www.page21.org).

94 | The most basic process in permafrost areas is the seasonal melting and freezing and thawing
95 | of soil water in the presence of continuously frozen ground below a certain depth. The
96 | response of the soil to freezing leads to specific variations in the annual cycle of soil
97 | hydrology. Frozen ground and snow cover also influence rainfall-runoff partitioning, the
98 | timing and magnitude of spring runoff, and the amount of soil moisture that subsequently is
99 | available for evapotranspiration in spring and summer ([Beer et al., 2006](#); [Beer et al., 2007](#);
100 | Koren et al., 1999). Soil moisture controls the partitioning of the available energy into latent
101 | and sensible heat flux and conditions the amount of surface runoff. By controlling
102 | evapotranspiration, it is linking the energy, water and carbon fluxes (Koster et al., 2004;
103 | Dirmeyer et al., 2006; Seneviratne and Stöckli, 2008). Seneviratne et al. (2006) stated that a
104 | northward shift of climatic regimes in Europe due to climate change will result in a new
105 | transitional climate zone between dry and wet climates with strong land–atmosphere coupling
106 | in central and eastern Europe. They specifically highlight the importance of soil-moisture–
107 | temperature feedbacks (in addition to soil-moisture–precipitation feedbacks) for future
108 | climate changes over this region. A comprehensive review on soil moisture feedbacks is given

109 by Seneviratne et al. (2010).

110 Largely, soil moisture feedbacks to the atmosphere are confined to regions where the
111 evapotranspiration is moisture-limited. These are regions where the soil moisture is in the
112 transitional regime between the permanent wilting point (soil moisture content below which
113 the plants can not extract water from the soil by transpiration as the suction forces of the soil
114 are larger than the transpiration forces of the plants) and the critical soil moisture W_{crit} above
115 which plants transpire at the potential rate [imposed by the atmospheric conditions, i.e. the](#)
116 [potential evapotranspiration](#) (see, e.g., Fig. 5 in Seneviratne et al., 2010). In this respect, the
117 high-latitudes are usually excluded [from](#) those regions as they are considered to be
118 predominantly energy-limited (Teuling et al., 2009), and where the coupling between soil
119 moisture and the atmosphere does not play a role (Koster et al., 2004, 2006).

120 Note that in previous studies where an ESM's land surface model (LSM) was equipped with
121 cold region soil processes, effects of resulting model improvements usually have not been
122 directly considered in a coupled atmosphere-land context. Either simulated changes were only
123 considered in the LSM standalone mode (e.g. Ekici et al., 2014, 2015; Lawrence and Slater,
124 2005; Gouttevin et al., 2012; Slater et al., 1998), or changes between different LSM version
125 were not limited to cold region processes alone (Cox et al., 1999). [Only Takata and Kimoto](#)
126 [\(2000\) conducted a kind of precursor to our study who used a very coarse resolution](#)
127 [atmospheric GCM \(600 km resolution\), but they neither used large-scale observations to](#)
128 [evaluate the results of their study nor specifically addressed land-atmosphere feedbacks.](#) Thus,
129 [any](#) soil moisture feedbacks to the atmosphere related to cold region soil processes have
130 [generally](#) been neglected so far.

131 In the present study, we show that the implementation of cold region soil processes into the
132 ESM of the Max Planck Institute for Meteorology, MPI-ESM, has a pronounced impact on

133 the simulated terrestrial climate over the northern high latitudes, and that this is mainly related
134 to a positive soil moisture-precipitation feedback. Section 2 introduces the used ESM version
135 and the setup of the associated simulations, Section 3 discusses the main results over several
136 high latitude river catchments, followed by a summary and conclusions in Section 4.

137 **2 Model, data and methods**

138 **2.1 Model description**

139 In this study, the atmosphere and land components of the [Earth System Model](#)(ESM) of the
140 Max Planck Institute for Meteorology (MPI-M), MPI-ESM 1.1, are utilized that consist of the
141 atmospheric GCM ECHAM6.3 (Stevens et al., 2013) and its land surface scheme JSBACH
142 3.0 (Raddatz et al., 2007, Brovkin et al., 2009). Both models have undergone several further
143 developments since the version (ECHAM6.1/JSBACH 2.0) used for the Coupled Model
144 Intercomparison Project 5 (CMIP5; Taylor et al., 2012). Several bug fixes in the ECHAM
145 physical parameterizations led to energy conservation in the total parameterized physics and a
146 re-calibration of the cloud processes resulted in a medium range climate sensitivity of about 3
147 K. JSBACH 3.0 comprises several bug fixes, a new soil carbon model (Goll et al., 2015) and
148 a five layer soil hydrology scheme (Hagemann and Stacke, 2015) replaced the previous
149 bucket scheme. [These five layers correspond directly to the structure used for soil](#)
150 [temperatures and they are defined with increasing thickness \(0.065, 0.254, 0.913, 2.902, and](#)
151 [5.7 m\) down to a lower boundary at almost 10 m depth.](#) In addition, a permafrost-ready
152 version of JSBACH is considered (JSBACH-PF) in which physical processes relevant at high
153 latitude land regions have been implemented by Ekici et al. (2014). Most importantly, these
154 processes comprise the freezing and [melting-thawing](#) of soil moisture. Consequently, the
155 latent heat of fusion dampens the amplitude of soil temperature, infiltration is decreased when

156 the uppermost soil layer is frozen, soil moisture is bound in solid phase when frozen, and,
157 hence, cannot be transported vertically or horizontally. Dynamic soil thermal properties now
158 depend on soil texture as well as on soil water and ice contents. Dynamic soil hydraulic
159 properties that depend on soil texture and soil water content may decrease when soil moisture
160 freezes (such as, e.g., the hydraulic conductivity).are decreased when soil moisture is frozen.
161 Moreover a snow scheme has been implemented in which snow can now develop in up to five
162 layers while the current scheme only represents up to two layers. In the original snow scheme,
163 the snow is thermally growing down inside the soil, i.e. the snow cover becomes part of the
164 soil temperature layers so that soil temperatures are mixed with snow temperatures. In the
165 new scheme, snow is accumulated~~The latter also thermally lets the snow grow inside the soil~~
166 ~~(i.e. soil temperatures are mixed with snow temperatures), while the new scheme accumulates~~
167 ~~the snow~~ on top of the soil using snow thermal properties. Further, a homogeneous organic
168 top layer is added with a constant depth and specific thermal and hydraulic properties. Note
169 that in the following the term soil moisture generally refers to the liquid soil moisture if not
170 mentioned otherwise. In this respect, total soil moisture refers to the sum of liquid and frozen
171 soil moisture.

172 2.2 Experimental setup

173 Two ECHAM6.3/JSBACH simulations were conducted at T63 horizontal resolution (about
174 200 km) with 47 vertical layers in the atmosphere. They were forced by observed sea surface
175 temperature (SST) and sea ice from the AMIP2 (Atmospheric Model Intercomparison Project
176 2) dataset forduring 1970-2009 (Taylor et al., 2000). 1970-1988 are regarded as spin-up
177 ~~phase, so that~~ only the period 1989-2009 is considered for the analyses. The two simulations
178 are:

- 179 • ECH6-REF: Simulation with the standard version of JSBACH 3.0 with a fixed

180 vegetation distribution and using a separate upper layer reservoir for bare soil
181 evaporation as described in Hagemann and Stacke (2015). Note that the latter is
182 switched off by default in JSBACH 3.0 to achieve a better performance of simulated
183 primary productivity, which is not of interest in the present study.

- 184 • ECH6-PF: As ECH6-REF, but using JSBACH-PF.

185 Note that both simulations used initial values of soil moisture, soil temperature and snowpack
186 that were obtained from an offline-simulation (land only) using JSBACH (as in ECH6-REF)
187 forced with WFDEI data (Weedon et al., 2014).

188 **2.3 Calculation of internal model climate variability**

189 The internal climate variability of ECHAM6/JSBACH with respect to 20-year mean values
190 has been estimated from results of three 20-year, 5-member ensembles, in which the
191 ensembles used different land-atmosphere coupling setups (deVrese et al., 2016). Within each
192 ensemble, the model setup is identical but the simulations were started using slightly differing
193 initial conditions. Following the approach of Hagemann et al. (2009), we first calculated the
194 standard deviation of 20-year means for each ensemble, and then the spread for each model
195 grid box is defined as the maximum of the three ensemble standard deviations. This spread is
196 then used as an estimate of the model's internal climate variability. Thus, if simulated
197 differences between ECH6-PF and ECH6-REF are larger than this spread, they are considered
198 as robust and directly related to the introduction of cold region soil processes into JSBACH.

199 **2.4 Observational data**

200 We use climatological observed river discharges from the station network of the Global
201 Runoff Data Centre (Dümenil Gates et al., 2000). Near surface air (2m) temperature and
202 precipitation are taken from the [recent](#) global WATCH dataset of hydrological forcing data

203 | (WFDEI; Weedon et al., 2014). The WFDEI combine the daily statistics of the Interim re-
204 analysis of the European Centre for Medium-Range Weather Forecasts (ERA-Interim; Dee et
205 al., 2011) with the monthly mean observed characteristics of temperature from the Climate
206 Research Unit dataset TS2.1 (CRU; Mitchell and Jones, 2005) and precipitation from the
207 Global Precipitation Climatology Centre full dataset version 4 (GPCC; Fuchs et al., 2007).
208 For the latter, a gauge-undercatch correction following Adam and Lettenmaier (2003) was
209 used, which takes into account the systematic underestimation of precipitation measurements
210 that have an error of up to 10-50% (see, e.g. Rudolf and Rubel, 2005).

211 For an estimate of observed evapotranspiration (ET), we are using data from the LandFlux-
212 EVAL dataset. This new product was generated to compile multi-year global merged
213 benchmark synthesis products based on the analyses of existing land evapotranspiration
214 datasets (monthly time scale, time periods 1989-1995 and 1989-2005). The calculation and
215 analyses of the products are described in Mueller et al. (2013). In our study we are using the
216 diagnostic products available for the period 1989-2005 that are based on various observations,
217 i.e. from remote sensing, diagnostic estimates (atmospheric water-balance estimates) and
218 ground observations (flux measurements). Here, we considered the mean, minimum and
219 maximum of the respective diagnostic ensemble.

220 Surface solar irradiance (SSI; 2000-2010) is taken from the Clouds and Earth Radiation
221 Energy System (CERES; Kato et al., 2013) that provides surface solar radiation fluxes at
222 global scale derived from measurements onboard of the EOS Terra and Aqua satellites (Loeb
223 et al., 2012). We used surface albedo data from MODIS (MCD43C3, ver5; 2000-2011;
224 Cescatti et al., 2012), CERES (2000-2010) and the GlobAlbedo project (1998-2011; Muller et
225 al., 2012) of the European Space Agency (ESA). With regard to the accumulated snowpack,
226 we compared model data to snow water equivalent data from the ESA GlobSnow project

227 (Takala et al., 2011), NASA's Modern-Era Retrospective Analysis for Research and
228 Applications (MERRA; 1979-2013; Rienecker et al., 2011) and the snow data climatology
229 (SDC) of Foster and Davy (1988).

230 **2.5 Permafrost extent**

231 Observational datasets of permafrost extent usually give three or four classes of spatial
232 permafrost occurrence, where the respective percentage of permafrost covered area is > 90 %
233 ('continuous'), between 90 and 50 % ('discontinuous'), < 50 % ('sporadic'), and, in some
234 references, < 10 % ('isolated'). This is the case in the data of Brown et al. (1997) shown here
235 in Fig. 1a. In most climate models, such a diversification of permafrost classes is not
236 possible. In those models as well as in JSBACH, soil temperatures are computed for one point
237 at the centre of a grid cell, thereby representing the whole area of that cell. Consequently, no
238 'non-continuous' permafrost can be computed by JSBACH. Thus, the comparison of simulated
239 with observed permafrost extents focuses on the continuous class in the observations.

240 In order to diagnose permafrost extent from JSBACH output, its fifth layer soil temperature
241 has been extracted and checked whether it has been lower than 0 °C for more than two years
242 in a row. This criterion was applied to a 30-year time series of monthly means (1979–2009),
243 and during every proceeding month, the sum of 'permafrost months' have been set into
244 relationship to the total number of months in the time series analysed so far. This enables us
245 to have temporal variation, and avoid 'loosing' permafrost areas where it simply did not occur
246 during the last two years of the analysed time series.

247 **3 Results**

248 Initially, the simulated permafrost extents are compared with the data of Brown et al. (1997)

249 | in Fig. 1. The implementation of permafrost relevant soil processes into JSBACH leads to an
250 | improved permafrost representation in terms of continuous permafrost extent, as the too large
251 | extent in western Siberia as well as in Alaska decreases in ECH-PF. Reasons for this
252 | improvement are presumably the changed snow scheme and the separation of snow and soil
253 | temperatures on the one hand, and the new formulation of the soil thermal properties on the
254 | other hand. Combined with the organic top layer, they change the conditions for heat transfer
255 | into and within the ground, which leads to more realistic deep soil temperatures in the above
256 | mentioned regions.

257 | Then, both The simulations ECH6-REF and ECH6-PF are evaluated over the northern high
258 | latitudes analogously to how the evaluation of surface water and energy fluxes of the CMIP5
259 | version of MPI-ESM was conducted by Hagemann et al. (2013b). The main differences in
260 | precipitation and 2m temperature between both simulations occur in the boreal summer. In
261 | ECH6-PF, precipitation is generally reduced compared to ECH~~6~~-REF over the northern high
262 | latitudes (Fig. 1Fig. 2). On the one hand, this leads to a general reduction of the wet bias
263 | compared to WFDEI data over the more continental areas north of about 60°N, especially
264 | over Canada and Russia. On the other hand, it enhances the dry bias over the adjacent mid-
265 | latitudes. Note that this summer dry bias of MPI-ESM 1.1 over mid-latitudes is more
266 | pronounced and wide-spread than in the CMIP5 version of MPI-ESM (cf. Fig. 4, middle row,
267 | in Hagemann et al., 2013b), which is likely associated with bug-fixes or the re-calibration of
268 | cloud processes in ECHAM6.3 (cf. Sect. 2.1). The same is also the case for northern
269 | hemisphere summer warm biases in ECH6-REF (Fig. 2Fig. 3). These warm biases are
270 | enhanced in ECH6-PF. This enhancement is partly related to the fact that the reduced
271 | precipitation is accompanied by a reduced cloud cover, and, hence an increased incoming
272 | solar radiation at the land surface (Fig. 3Fig. 4). Compared to CERES data, the low bias in
273 | SSI over the high latitudes is largely removed while the overestimation over the mid-latitudes

274 is slightly increased. The reason for the warmer air temperatures can partly be found in a
275 decreased evapotranspiration (ET) when permafrost relevant physical soil processes are
276 switched on. A detailed analysis of their effects was carried out to elucidate the specific
277 influence of these processes and is shown for two large example catchments ([Fig. 4](#)[Fig. 5](#)). 1)
278 The Arctic catchment is represented by the six largest rivers flowing into the Arctic Ocean:
279 Kolyma, Lena, Mackenzie, Northern Dvina, Ob and Yenisei. The associated catchments
280 comprise a large fraction of permafrost covered areas ([cf. Fig. 1](#)). 2) The Baltic Sea catchment
281 includes only a low amount of permafrost covered areas but soil moisture freezing still plays a
282 role over large parts of the catchment during the winter.

283 *Arctic River catchments*

284 ECH6-PF simulates the discharge of the six largest Arctic rivers more reliably than ECH6-
285 REF, especially with regard to timing and size of the snow melt induced discharge peak in
286 spring ([Fig. 5](#)[Fig. 6a](#)). This is largely related to the fact that in ECH6-PF, a major part of the
287 snow melt turns into surface runoff as it cannot infiltrate into the ground when this is still
288 frozen in the beginning of spring. This is opposite to ECH6-REF where larger parts of the
289 snow melt are infiltrating into the soil due to the missing freezing processes such that the
290 observed discharge peak is largely underestimated.

291 Consistent with Fig. 1, Also with regard to precipitation, ECH6-PF shows a large
292 improvement in the simulated summer precipitation as the large wet bias in the summer
293 precipitation of ECH6-REF is strongly reduced and, hence, much closer to WFDEI data in
294 ECH6-PF ([Fig. 5](#)[Fig. 6c](#)). This reduction in summer precipitation is accompanied by a
295 reduction in summer evapotranspiration ([Fig. 6](#)[Fig. 7a](#)) that is now much closer to the mean of
296 diagnostic estimates from the LandFlux dataset, while it is likely overestimated in ECH6-REF
297 as the simulated evapotranspiration is close to the upper limit of the LandFlux diagnostic

estimates. This ET reduction in ECH6-PF is directly related to a completely changed seasonal cycle of liquid relative soil moisture (actual soil moisture divided by the maximum soil water holding capacity) in the root zone (Fig. 6 Fig. 7c). In ECH6-REF, the soil is very wet throughout the whole year with somewhat lower values in summer that are related to the summer ET. In ECH6-PF, the soil is rather dry in winter as larger parts of the total soil moisture are frozen (Fig. 7 Fig. 8), and, hence, not accessible for ET. With infiltration of snowmelt in the spring when the soil water of the upper layer has meltedthawed, the soil moisture is increasing and reaches its maximum in summer. The total amount of liquid soil moisture in ECH6-PF is much lower than in ECH6-REF. On the one hand large parts of the soil are frozen in winter and adjacent months (Fig. 7 Fig. 8), and on the other hand this is related to the much lower infiltration in spring, so that less soil moisture is available throughout the whole year. In the autumn and winter, the amount of total amount of soil water moisture is somewhat increasing (Fig. 6 Fig. 7c) as due to freezing, it is locally bound and can neither flow off laterally nor evaporate. — If compared to the model's internal climate variability (Fig. 8 Fig. 9) we note that the differences between ECH6-PF and ECH6-REF are robust for ET and precipitation from April-October and April-August, respectively.

The decreased ET during warm months, however, brings about less evaporative cooling of the land surface and a reduced upward moisture flux into the atmosphere that in turn seems to reduce cloud cover, and, hence SSI is increased in ECH6-PF (Fig. 9c, see also Fig. 3). Both of these effects, and near surface air temperature increases with the use of the PF scheme. This results in a further increase of the summer warm bias in 2m air temperature in comparison to WFDEI data (Fig. 9 Fig. 10a, see also Fig. 2). Parts of the summer warm bias is caused by an overestimated incoming surface solar irradiance (SSI). In ECH6-REF, the simulated SSI is close to CERES data (Fig. 9 Fig. 10c), but in ECH6-PF the reduced ET leads to a reduced upward moisture flux into the atmosphere that in turn seems to reduce cloud cover, and, hence

323 | **SSI is increased.**

324 | The surface albedo is rather similar in both experiments ([Fig. 10](#)[Fig. 11a](#)) but shows some
325 | distinct biases if compared to various observational datasets. During the winter JSBACH
326 | seems to overestimate the mainly snow-related albedo, indicating that it may have difficulties
327 | to adequately represent snow-masking effect of boreal forests [¶](#)[Note that a version of MODIS
328 | albedo data was used where low quality data over the very high northern latitudes were
329 | filtered out in the boreal winter due to too low available radiation (A. Löw, pers. comm.,
330 | 2016). Due to these missing data over mainly snow covered areas, MODIS albedo averaged
331 | over the six largest Arctic rivers is biased low in the winter[¶](#).] During the summer, there is a
332 | larger uncertainty in the observations. While the simulated albedo is close to MODIS and
333 | CERES data, it is lower than GlobAlbedo data. As a too low albedo would lead to a warm
334 | bias, this might indicate a better reliability of the GlobAlbedo data for this region in summer.
335 | Note that a sensitivity test where surface albedo was increased by 0.05 north of 60°N led to a
336 | reduction of the warm bias by about 1-2 K (not shown). As already indicated by the surface
337 | albedo, the simulated snow cover does not significantly differ between the experiments, either
338 | ([Fig. 10](#)[Fig. 11c](#)). It is lower than various observational estimates, which should impose a low
339 | albedo bias in winter. As this bias is in the opposite direction, it can be concluded that the low
340 | snow pack is compensating part of the snow masking problem mentioned above.

341 | **Baltic Sea catchment**

342 | A similar effect of the frozen ground is found over the Baltic Sea catchment, although this is
343 | less strong than for the Arctic rivers. The frozen ground leads to an enhanced snow melt
344 | runoff in spring ([Fig. 5](#)[Fig. 6b](#)) and a less strong replenishment of the ground by water during
345 | the winter as it is the case for ECH6-REF ([Fig. 6](#)[Fig. 7d](#)). Consequently the average level of
346 | liquid soil moisture is lower in ECH6-PF compared to ECH6-REF. This leads to more

347 infiltration of water and less drainage, and hence, less runoff in the summer, which in turns
348 leads to an improved simulation of discharge ([Fig. 5](#)[Fig. 6b](#)). The impact on the atmosphere is
349 much less pronounced than for the Arctic rivers. On one hand there is less frozen ground in
350 the Baltic Sea catchment ([Fig. 7](#)[Fig. 8](#)), on the other hand the average soil moisture content is
351 larger than for the Arctic rivers ([Fig. 6](#)[Fig. 7d](#)). In ECH6-REF, the soil moisture is generally
352 above W_{crit} (c.f. Sect. 1) [ever_in](#) the Baltic Sea catchment so that ET is largely energy limited
353 and mostly occurring at its potential rate. Even though the ECH6-PF soil moisture is lower, it
354 is generally still close to W_{crit} so that ET is only slightly reduced, especially in the second half
355 of the year ([Fig. 6](#)[Fig. 7b](#)). Precipitation is also somewhat reduced ([Fig. 5](#)[Fig. 6d](#)) but this
356 seems to be mostly related to the internal climate variability except for September and
357 October when a somewhat stronger and robust reduction in ET leads to a robust precipitation
358 decrease ([Fig. 8](#)[Fig. 9](#)).

359 4 Discussion and conclusions

360 The results described in the previous section show that ~~the introduction of cold region~~
361 ~~processes into MPI-ESM led to a soil freezing and thawing processes enable the~~ positive soil
362 moisture-precipitation feedback ([e.g. Dirmeyer et al., 2006; Seneviratne et al., 2010](#)) over
363 large parts of northern mid- and high latitudes during the boreal summer. The chain of
364 processes leading to [and influencing](#) this feedback is sketched in [Fig. 11](#)[Fig. 12](#). The frozen
365 soil during the cold season (late autumn to early spring) leads to less infiltration of rainfall
366 and snowmelt during this season, and, hence, to more surface runoff especially during the
367 snowmelt period. On one hand this leads to a large improvement in simulated discharge,
368 mainly due to the improved snowmelt peak. This improved discharge due to the
369 representation of frozen ground has been also reported for other models (Beer et al., 2006,
370 2007; Ekici et al., 2014; Gouttevin et al., 2012). On the other hand, this leads to a decrease of

371 soil moisture. [This spring soil moisture deficit from the increased discharge extents into](#)
372 [During the boreal summer due to the soil moisture memory \(e.g. Koster and Suarez 2001,](#)
373 [Orth and Seneviratne 2012\), when it, this](#) actually causes more infiltration and less runoff,
374 and, hence, less discharge. The latter strongly improves the simulated discharge in the Baltic
375 Sea catchment from summer to early winter. The decreased soil moisture leads to a reduced
376 ET in regions where the soil moisture is in the transitional regime. Here, there is less
377 recycling of moisture into the atmosphere, and the lower atmospheric moisture causes a
378 reduction of precipitation that in turn leads to a further reduction of soil moisture.

379 [Our new finding of the importance of the positive soil moisture-precipitation feedback in](#)
380 [northern high latitudes has been supported by correlations between soil moisture and](#)
381 [precipitation using monthly values from 1989-2009. While there are higher correlations](#)
382 [between soil moisture and precipitation in the mid-latitudes for ECH6-REF \(Fig. 12a\), the](#)
383 [high latitudes are mostly characterized by rather low correlations using the reference version](#)
384 [of JSBACH. Figure 13b and c show that the correlation between soil moisture and](#)
385 [precipitation is strongly increased in ECH6-PF over large parts of the northern high latitudes,](#)
386 [especially over North America and eastern Siberia. This confirms an increased coupling of](#)
387 [soil moisture and precipitation, and, hence, also indicates that the soil moisture-precipitation](#)
388 [feedback is highly enabled in these areas.](#) This positive soil moisture-precipitation feedback
389 improves the simulated hydrological cycle, especially over the Arctic rivers where the wet
390 biases in summer precipitation and ET are reduced. Less ET, and, hence, less evaporative
391 cooling cause an increase in summer 2m air temperatures. This, in combination with more
392 incoming surface solar radiation due to fewer clouds, increases and extends the existing
393 summer warm bias of MPI-ESM north of about 50°N. [Since air temperature is a main driver](#)
394 [of soil freezing and thawing processes, there are more indirect interactions between energy](#)
395 [and water balances which call for even more advanced factorial model experiments in the](#)

396 future.

397 Changes in the simulated hydrological cycle induced by the utilization of the improved soil
398 scheme are mostly confined to areas where freezing and thawing of water play a role. To
399 illustrate this, Fig. 13 shows the number of months where in the climatological average of
400 1989-2009, the upper soil layer is below 0°C in ECH6-PF. Changes in precipitation (Fig. 1)
401 and surface solar irradiance (Fig. 3), indicating changes in cloud cover, are mostly located in
402 regions where the upper layer is frozen for at least three months within the climatological
403 average. Changes outside of regions with soil frost may be imposed by changed atmospheric
404 humidity and heat transport from soil frost affected regions on the one hand. On the other
405 hand, Ekici et al. (2014) also introduced a permanent, static organic top layer as part of the
406 new JSBACH-PF soil scheme. If switched on, as in the current ECH6-PF simulation, it is
407 considered globally uniform, thus introducing a soil isolating effect also outside permafrost
408 regions. As a consequence, the partitioning of the surface heat balance is altered during snow-
409 free months towards a decreased ground heat flux, which needs to be compensated for by the
410 turbulent heat fluxes, in particular by the sensible heat flux. This in turn contributes to the
411 warming of the 2m air temperature which can be seen also in areas without any soil frost (Fig.
412 2). Even though the uniform organic insulation layer was implemented globally, Fig. 12
413 shows that the correlation between soil moisture and precipitation advances strongly in
414 northern high latitudes only while this correlation has nearly not changed in the temperate
415 zone and in particular in drought-dominated areas in south-east Europe or mid-west USA.
416 Note that currently, the land surface scheme has been further advanced by a mechanistic
417 model of mosses and lichens dynamics (Porada et al., 2016) which will replace the actual
418 static organic top layer for soil insulation. This will enable a more realistic representation of
419 the temporal and spatial variation of the soil insulation.

Such-aA positive soil moisture-precipitation feedback has not been pointed out for the northern high latitudes so far, even though in their coarse resolution GCM study, Takata and Kimoto (2000) found similar impacts to those shown in Fig. 11 induced by soil water freezing. Previously, the northern high latitudes which previously have generally been considered as energy-limited regimes where land-atmosphere coupling due to soil moisture does not play a role (e.g. Teuling et al., 2009). But this principal feedback loop has been found for drier regions where the soil moisture is generally in the transitional regime and land-atmosphere coupling plays a role. Koster et al. (2004) considered the strength of coupling between soil moisture and precipitation in an ensemble of atmospheric GCMs. The resulting map is very similar to the map regarding the strength of coupling between soil moisture and temperature in the same GCMs (Koster et al., 2006). This suggests that in these models, the same process controls both couplings, namely the ET sensitivity to soil moisture that leads to a positive feedback (Seneviratne et al., 2010). But on the one hand it can be assumed that many models participating in those earlier studies did not include the freezing and thawing of soil water. Thus, our reference simulation ECH6-REF is in line with results reported in the literature, generally not showing a strong coupling between precipitation and soil moisture in permafrost regions, such as indicated by the rather low correlation values in Fig. 12a. Only the ECH6-PF simulation using advanced soil physics shows that such strong coupling indeed is present (Fig. 12b). On the other hand, only annual mean diagnostics were considered in some of those earlier studies (e.g. Teuling et al., 2009). In other land-atmosphere coupling studies, that, e.g., followed the GLACE protocol such as Koster et al. (2004), prescribed soil moisture conditions were used that were similar to the average soil moisture climatology. Here, it seems that the differences between the simulations with free and prescribed soil moisture in GLACE type simulations may be not large enough to reveal a large-scale feedback over the high latitudes. This may only be possible by an experimental

445 design where more pronounced summer soil moisture changes are introduced. Note that in the
446 present study, these pronounced changes were introduced not due to an artificial design, but
447 they were caused by the implementation of previously missing frozen soil physics into the
448 model. But in those studies (Koster et al., 2004; Teuling et al., 2009), usually annual mean
449 diagnostics were considered. Our study has shown that spring moisture deficits can lead to
450 seasonally, i.e. during the boreal summer, soil moisture conditions during the boreal summer
451 may prevail that allow for an advanced land-atmosphere coupling and a positive soil
452 moisture-precipitation feedback over the northern high and mid latitudes.

453 Even though our results are obtained with a modelling study, their physical consistency
454 suggests that cold region soil processes, especially melting and freezing and thawing of soil
455 moisturewater, may lead to a positive soil moisture precipitation feedback during the summer
456 in reality, too. A prerequisite for the occurrence of a soil moisture precipitation feedback is
457 that soil moisture is in the transitional regime. Thus, the strength of the feedback depends on
458 the wetness of the soil and, hence, is likely model dependent. Models with wetter/drier soils
459 over the considered regions may simulate a weaker/stronger feedback.

460 Several modelling studies pointed out that there are not only positive feedback loops between
461 soil moisture and precipitation but also negative ones that, under specific conditions, such as
462 convective instability and/or cloud formation, may be stronger over dry soils (e.g.
463 Hohenegger et al., 2009; Froidevaux et al., 2014). However, to date, the latter results appear
464 mostly confined to single-column, cloud-resolving, and some high-resolution regional climate
465 simulations (Seneviratne et al., 2010) and may also depend on the choice of the convective
466 parameterisations (e.g. Giorgi et al., 1996). Guillod et al. (2015) noted that precipitation
467 events tend to be located over drier patches, but they generally need to be surrounded by wet
468 conditions; positive temporal soil moisture-precipitation relationships are thus driven by

469 large-scale soil moisture. Thus, negative feedbacks seem to have more an impact on high
470 resolution and thus on the local scale (Ho-Hagemann et al., 2015), where the effects of land
471 surface heterogeneity for the inferred feedbacks also need to be taken into account (Chen and
472 Avissar, 1994; Pielke et al., 1998; Taylor et al., 2013). Consequently most GCMs may not be
473 able to represent negative feedbacks between soil moisture and precipitation via ET. As in the
474 present study, we considered the effect of large-scale soil moisture changes due to soil
475 freezing processes, the identification of potential negative feedbacks on the local scale is
476 beyond the scope of the present study~~not an issue~~.

477 In MPI-ESM, an unwelcome effect of implementing cold region soil processes is the increase
478 of the existing warm bias over the high latitudes during summer. In order to estimate the
479 contribution of biases in SSI and surface albedo to this warm bias, we calculated an upper
480 limit for the temperature change that may be imposed by a radiation difference in the related
481 energy flux into the ground [$\text{SSI} \times (1 - \text{albedo})$]. For this estimation we assume that the
482 surface temperature is adjusting in a way that this radiation difference is compensated by
483 thermal radiation following the Stefan Boltzmann law. Here, any change in the turbulent
484 surface heat fluxes is neglected so that the resulting temperature change is an upper limit for
485 the temperature bias that might be explained by a radiation bias.

486 Considering the mean summer biases over the six largest Arctic rivers (Table 1) indicates that
487 a part of the warm bias may be attributed to the overestimation in SSI. For ECH6-PF (ECH6-
488 REF), the SSI bias may cause a warm bias of up to 2.9 K (0.9 K). The surface albedo may
489 contribute another 0.7 K (0.8 K) to the warm bias if compared to GlobAlbedo data but this is
490 a rather vague estimation due to the large uncertainty on surface albedo observations (see [Fig.](#)
491 [10](#)[Fig.](#)[11](#)). Nevertheless biases in both of these variables cannot explain the full bias of 5 K
492 (2.1 K) in 2m temperature. Further contributions to this warm bias might be related to [too](#)

493 ~~much advection of warm air or~~ a too weak vertical mixing of heat within the boundary layer.
494 ~~or too much advection of warm air. The latter may also influence the recycling ratio of water~~
495 ~~within and outside regions of soil frost.~~ A deeper investigation of this is beyond the scope of
496 the present study and should be dealt with in future model improvements.

497 We have shown that ~~biosoil~~ physical ~~land surface~~ processes such as ~~melting-thawing~~ and
498 freezing ~~can~~ have an ~~significant~~ impact on the regional climate over the high latitudes~~s and~~
499 permafrost areas. Flato et al. (2013) reported that CMIP5 GCMs tend to overestimate
500 precipitation over northern high latitudes except for Europe and western Siberia. As many of
501 these GCMs are still missing basic cold region processes (see Sect. 11), a missing ~~interaction~~
502 ~~between~~ soil moisture ~~and~~ precipitation ~~feedback~~ in those GCMs ~~might is likely to~~ contribute
503 to this wet bias. ~~Beyond the biophysical coupling between land and atmosphere, the coupling~~
504 ~~to biogeochemistry, i.e. vegetation and carbon cycle including methane and frozen carbon, is~~
505 ~~important to quantify feedbacks related to wetlands and permafrost over those areas. The~~
506 ~~representation of their complex dynamics within ESMs is a challenging task, but it is~~
507 ~~nevertheless necessary to investigate on-going and future climate changes over the high-~~
508 ~~latitude regions. Thus, the~~An adequate implementation of physical soil processes into an ESM
509 is only the first necessary step to yield an adequate representation of ~~climate feedbacks~~land-
510 atmosphere interactions over the high latitudes. This also includes the incorporation of
511 wetland dynamics, which will be the next step in the JSBACH development with regard to
512 high latitudes, thereby following an approach of Stacke and Hagemann (2012). In addition, a
513 reliable hydrological scheme for permafrost regions will allow investigations of related
514 climate-carbon cycle feedback mechanisms (McGuire et al., 2006; Beer, 2008; Heimann and
515 Reichstein, 2008).
516 Our findings demonstrate that soil freezing and thawing induce a much stronger coupling of

517 land and atmosphere in northern high latitudes than previously thought. The additional
518 importance of the positive soil moisture precipitation feedback in high latitudes will have a
519 strong impact on future climate projections in addition to other biophysical (e.g. albedo) or
520 biogeochemical (e.g. climate-carbon cycle) feedback mechanisms. Therefore, the findings of
521 this study additionally highlight the importance of permafrost ecosystem functions in relation
522 to climate.

523 **Acknowledgments**

524 The authors acknowledge the financial support of T. Blome by the European Union FP7-ENV
525 project PAGE21 under contract number GA282700. S. Hagemann is supported by funding
526 from the European Union within the Horizon 2020 project CRESCENDO (grant no. 641816).

527 **References**

528 ACIA: Arctic Climate Impact Assessment, Cambridge University Press, 1042p.,
529 <http://www.acia.uaf.edu>, 2005.

530 Adam, J. C., and, Lettenmaier, D. P.: Adjustment of global gridded precipitation for
531 systematic bias, J. Geophys. Res., 108, D9, 4257, doi:10.1029/2002JD002499, 2003.

532 Beer, C.: Soil science: The Arctic carbon count. Nature Geoscience, 1, 569-570,
533 doi:10.1038/ngeo292, 2008.

534 Beer, C., Lucht, W., Schmullius, C., and Shvidenko, A.: Small net carbon dioxide uptake by
535 Russian forests during 1981–1999, Geophys. Res. Lett., 33, L15403,
536 doi:10.1029/2006GL026919, 2006.

537 Beer, C., Lucht, W., Gerten, D., Thonicke, K., and Schmullius, C.: Effects of soil freezing and
538 thawing on vegetation carbon density in Siberia: A modeling analysis with the Lund-

- 539 Potsdam-Jena Dynamic Global Vegetation Model (LPJ-DGVM), Global Biogeochem.
540 Cyc., 21, GB1012, doi:10.1029/2006GB002760, 2007.
- 541 Brovkin, V., Raddatz, T., Reick, C. H., Claussen, M., and Gayler, V.: Global biogeophysical
542 interactions between forest and climate, Geophys. Res. Letters, 36, L07 405,
543 doi:10.1029/2009GL037543, 2009.
- 544 Brown, J., Ferrians Jr., O. J., Heginbottom, J. A., and Melnikov, E. S. (eds.): Circum-Arctic
545 map of permafrost and ground-ice conditions, Washington, DC: U.S. Geological Survey
546 in Cooperation with the Circum-Pacific Council for Energy and Mineral Resources.
547 Circum-Pacific Map Series CP-45, scale 1:10,000,000, 1997.
- 548 Cescatti, A., Marcolla, B., Santhana Vannan, S. K., Pan, J. Y., Román, M. O., Yang, X.,
549 Ciais, P., Cook, R. B., Law, B. E., Matteucci, G., Migliavacca, M., Moors, E.,
550 Richardson, A. D., Seufert, G., and Schaaf, C.B.: Intercomparison of MODIS albedo
551 retrievals and in situ measurements across the global FLUXNET network, Rem. Sens.
552 Environ., 121, 323-334, 2012.
- 553 Chen, F., and Avissar, R.: Impact of land-surface moisture variability on local shallow
554 convective cumulus and precipitation in large-scale models, J. Appl. Meteorol., 33 (12),
555 1382–1401, 1994.
- 556 Cox, P., Betts, R., Bunton, C., Essery, R., Rowntree, P., and Smith, J.: The impact of new
557 land surface physics on the GCM simulation. of climate and climate sensitivity, Climate
558 Dyn., 15, 183–203, doi:10.1007/s003820050276, 1999.
- 559 de Vrese, P., and Hagemann, S.: Explicit representation of spatial sub-grid scale heterogeneity
560 in an ESM, J. Hydrometeorol., submitted, 2016.
- 561 Dee, D. P., Uppala, S. M., Simmons, A. J., Berrisford, P., Poli, P., Kobayashi, S., Andrae, U.,
562 Balmaseda, M. A., Balsamo, G., Bauer, P., Bechtold, P., Beljaars, A. C. M., van de Berg,

- 563 L., Bidlot, J., Bormann, N., Delsol, C., Dragani, R., Fuentes, M., Geer, A. J., Haimberger,
564 L., Healy, S. B., Hersbach, H., Hólm, E. V., Isaksen, L., Kållberg, P., Köhler, M.,
565 Matricardi, M., McNally, A. P., Monge-Sanz, B. M., Morcrette, J.-J., Park, B.-K.,
566 Peubey, C., de Rosnay, P., Tavolato, C., Thépaut, J.-N., and Vitart, F.: The ERA-interim
567 reanalysis: configuration and performance of the data assimilation system, *Q. J. Roy.*
568 Meteorol. Soc., 137, 553–597, doi:10.1002/qj.828, 2011.
- 569 Dirmeyer, P., Koster, R., and Guo, Z. A. D.: Do global models properly represent the
570 feedback between land and atmosphere?, *J. Hydrometeorol.*, 7, 1177–1198, 2006.
- 571 Dümenil Gates, L., Hagemann, S., and Golz, C.: Observed historical discharge data from
572 major rivers for climate model validation, Max Planck Institute for Meteor. Rep., 307
573 [available from MPI for Meteorology, Bundesstr. 53, 20146 Hamburg, Germany], 2000.
- 574 Ekici, A., Beer, C., Hagemann, S., Boike, J., Langer, M., and Hauck, C.: Simulating high
575 latitude permafrost regions by the JSBACH terrestrial ecosystem model, *Geosci. Model*
576 *Dev.*, 7, 631–647, doi:10.5194/gmd-7-631-2014, 2014.
- 577 Ekici, A., Chadburn, S., Chaudhary, N., Hajdu, L. H., Marmy, A., Peng, S., Boike, J., Burke,
578 E., Friend, A. D., Hauck, C., Krinner, G., Langer, M., Miller, P. A., and Beer, C.: Site-
579 level model intercomparison of high latitude and high altitude soil thermal dynamics in
580 tundra and barren landscapes, *The Cryosphere*, 9, 1343–1361, doi:10.5194/tc-9-1343-
581 2015, 2015.
- 582 Flato, G., Marotzke, J., Abiodun, B., Braconnot, P., Chou, S. C., Collins, W., Cox, P.,
583 Driouech, F., Emori, S., Eyring, V., Forest, C., Gleckler, P., Guilyardi, E., Jakob, C.,
584 Kattsov, V., Reason, C., and Rummukainen, M.: Evaluation of Climate Models. In:
585 Climate Change 2013: The Physical Science Basis, Contribution of Working Group I to
586 the Fifth Assessment Report of the Intergovernmental Panel on Climate Change [Stocker,

- 587 T.F., Qin, D., Plattner, G.-K., Tignor, M., Allen, S. K., Boschung, J., Nauels, A., Xia, Y.,
588 Bex, V., and Midgley, P. M. (eds.)]. Cambridge University Press, Cambridge, United
589 Kingdom and New York, NY, USA, 2013.
- 590 Foster, D. J., and Davy, R.D.: Global snow data climatology, USAFETAC/TN-88/006, Scott
591 Air Force Base III, 1988.
- 592 French, H. M.: Editorial, Permafrost Periglac. Process, 1, 1, doi: 10.1002/ppp.3430010102,
593 1990.
- 594 Froidevaux, P., Schlemmer, L., Schmidli, J., Langhans, W., and Schär, C.: Influence of
595 background wind on the local soil moisture-precipitation feedback, J. Atmos. Sci., 71,
596 782-799, 2014.
- 597 Fuchs, T., Schneider, U., and Rudolf, B.: Global Precipitation Analysis Products of the
598 GPCC, Global Precipitation Climatology Centre (GPCC). Deutscher Wetterdienst,
599 Offenbach, Germany, 2007.
- 600 Giorgi, F., Mearns, L.O., Shields, C., and Mayer, L.: A regional model study of the
601 importance of local versus remote controls of the 1988 drought and the 1993 flood over
602 the central United States, J. Climate, 9, 1150–1162, 1996.
- 603 Goll, D. S., Brovkin, V., Liski, J., Raddatz, T., Thum, T., and Todd-Brown, K. E. O.: Strong
604 dependence of CO₂ emissions from anthropogenic land cover change on initial land cover
605 and soil carbon parametrization, Global Biogeochem. Cycles, 29, 1511–1523,
606 doi:10.1002/2014GB004988, 2015.
- 607 Gouttevin, I., Krinner, G., Ciais, P., Polcher, J., and Legout, C.: Multi-scale validation of a
608 new soil freezing scheme for a land-surface model with physically-based hydrology, The
609 Cryosphere, 6, 407-430, doi:10.5194/tc-6-407-2012, 2012.
- 610 Guillod, B. P., Orlowsky, B., Miralles, D. G., Teuling, A. J., and Seneviratne, S. I.:

- 611 Reconciling spatial and temporal soil moisture effects on afternoon rainfall, Nat.
612 Commun., 6, 6443, doi: 10.1038/ncomms7443, 2015.
- 613 Hagemann, S., Göttel, H., Jacob, D., Lorenz, P., and Roeckner, E.: Improved regional scale
614 processes reflected in projected hydrological changes over large European catchments,
615 Climate Dyn., 32, 767-781, doi: 10.1007/s00382-008-0403-9, 2009.
- 616 Hagemann, S., Blome, T., Saeed, F., and Stacke, T.: Perspectives in modelling climate-
617 hydrology interactions, Surveys in Geophys., 35, 739-764, ISSI special issue on
618 Hydrological Cycle, doi:10.1007/s10712-013-9245-z, 2013a.
- 619 Hagemann, S., Loew, A., Andersson, A.: Combined evaluation of MPI-ESM land surface
620 water and energy fluxes, J. Adv. Model. Earth Syst., 5, doi:10.1029/2012MS000173,
621 2013b.
- 622 Hagemann, S., and Stacke, T.: Impact of the soil hydrology scheme on simulated soil
623 moisture memory, Climate Dyn., 44, 1731-1750, doi:10.1007/s00382-014-2221-6, 2015.
- 624 [Heimann, M., and Reichstein, M.: Terrestrial ecosystem carbon dynamics and climate](#)
625 [feedbacks, Nature, 451, 289-292, 2008.](#)
- 626 Ho-Hagemann, H. T. M., Rockel, B., and Hagemann, S.: On the role of soil moisture in the
627 generation of heavy rainfall during the Oder flood event in July 1997, Tellus A, 67,
628 28661, dx.doi.org/10.3402/tellusa.v67.28661, 2015.
- 629 Hohenegger, C., Brockhaus, P., Bretherton, C. S., and Schär, C.: The Soil Moisture–
630 Precipitation Feedback in Simulations with Explicit and Parameterized Convection, J.
631 Climate, 22, 5003–5020, 2009.
- 632 [Hugelius, G., Strauss, J., Zubrzycki, S., Harden, J. W., Schuur, E. A. G., Ping, C.-L.,](#)
633 [Schirrmeister, L., Grosse, G., Michaelson, G. J., Koven, C. D., O'Donnell, J. A.,](#)
634 [Elberling, B., Mishra, U., Camill, P., Yu, Z., Palmtag, J., and Kuhry, P.: Estimated stocks](#)

635 of circumpolar permafrost carbon with quantified uncertainty ranges and identified data
636 gaps, Biogeosciences, 11, 6573-6593, doi:10.5194/bg-11-6573-2014, 2014.

637 Kato, S., Loeb, N. G., Rose, F. G., Doelling, D. R., Rutan, D. A., Caldwell, T. E., Yu, L., and
638 Weller, R. A.: Surface irradiances consistent with CERES-derived top-of-atmosphere
639 shortwave and longwave irradiances, J. Climate, 26, 2719-2740, doi: 10.1175/JCLI-D-12-
640 00436.1, 2013.

641 Koren, V., Schaake, J., Mitchell, K., Duan, O. Y., Chen, F., and Baker, J. M.: A
642 parameterization of snowpack and frozen ground intended for NCEP weather and climate
643 models, J. Geophys. Res., 104, 19569–19585, 1999.

644 Koster, R. D., and Suarez, M. J.: Soil moisture memory in climate models. J. Hydrometeorol.,
645 2, 558-570, 2001.

646 Koster, R. D., Dirmeyer, P. A., Guo, Z., Bonan, G., Chan, E., Cox, P., Gordon, C. T., Kanae,
647 S., Kowalczyk, E., Lawrence, D., Liu, P., Lu, C. H., Malyshev, S., McAvaney, B.,
648 Mitchell, K., Mocko, D., Oki, T., Oleson, K., Pitman, A., Sud, Y. C., Taylor, C. M.,
649 Verseghy, D., Vasic, R., Xue, Y., and Yamada, T.: Regions of strong coupling between
650 soil moisture and precipitation, Science, 305, 1138–1140, 2004.

651 Koster R. D., Guo, Z., Dirmeyer, P. A., Bonan,, G., Chan, E., Cox, P., Davies, H., Gordon, C.
652 T., Kanae, S., Kowalczyk, E., Lawrence, D., Liu, P., Lu, C. H., Malyshev, S., McAvaney,
653 B., Mitchell, K., Mocko, D., Oki, T., Oleson, K. W., Pitman, A., Sud, Y. C., Taylor, C.
654 M., Verseghy, D., Vasic, R., Xue, Y., and Yamada, T.: GLACE: The Global Land-
655 Atmosphere Coupling Experiment. Part I: Overview, J. Hydrometeorol., 7, 590–610,
656 2006.

657 Koven, C. D., Riley, W. J., and Stern, A.: Analysis of permafrost thermal dynamics and
658 response to climate change in the CMIP5 Earth System Models, J. Climate, 26, 1877-

- 659 1900, doi:10.1175/JCLI-D-12-00228.1, 2012.
- 660 Lawrence, D. M., and Slater, A. G.: A projection of severe near-surface permafrost
661 degradation during the 21st century, *Geophys. Res. Lett.*, 32, L24401,
662 doi:10.1029/2005GL025080, 2005.
- 663 Loeb, N. G., Kato, S., Su, W., Wong, T., Rose, F. G., Doelling, D. R., and Norris, J.:
664 Advances in understanding top-of-atmosphere radiation variability from satellite
665 observations, *Surveys in Geophysics*, doi: 10.1007/s10712-012-9175-1, 2012.
- 666 Luo, L. F., Robock, A., Vinnikov, K. Y., Schlosser, C. A., Slater, A. G., Boone, A., Braden,
667 H., Cox, P., de Rosnay, P., Dickinson, R. E., Dai, Y. J., Duan, Q. Y., Etchevers, P.,
668 Henderson-Sellers, A., Gedney, N., Gusev, Y. M., Habets, F., Kim, J. W., Kowalczyk, E.,
669 Mitchell, K., Nasonova, O. N., Noilhan, J., Pitman, A. J., Schaake, J., Shmakin, A. B.,
670 Smirnova, T. G., Wetzel, P., Xue, Y. K., Yang, Z. L., and Zeng, Q. C.: Effects of frozen
671 soil on soil temperature, spring infiltration, and runoff: Results from the PILPS 2(d)
672 experiment at Valdai, Russia, *J. Hydrometeorol.*, 4, 334–351, 2003.
- 673 [McGuire, A.D., Chapin III, F.S., Walsh, J.E. and Wirth, C.: Integrated regional changes in](#)
674 [arctic climate feedbacks: Implications for the global climate system, Annu. Rev. Environ.](#)
675 [Resour. 31, 61–91, doi:10.1146/annurev.energy.31.020105.100253, 2006.](#)
- 676 [McGuire, A. D., Anderson, L. G., Christensen, T. R., Dallimore, S., Guo, L., Hayes, D. J.,](#)
677 [Heimann, M., Lorenson, T. D., Macdonald, R. W., and Roulet, N.: Sensitivity of the](#)
678 [carbon cycle in the Arctic to climate change, Ecological Monographs, 79, 523–555,](#)
679 [doi:10.1890/08-2025.1, 2009.](#)
- 680 Meehl, G. A., Boer, G. J., Covey, C., Latif, M., and Stouffer, R. J.: The Coupled Model
681 Intercomparison Project (CMIP), *Bull. Amer. Meteor. Soc.*, 81, 313–318, 2000.
- 682 Mitchell, T. D., and Jones, P. D.: An improved method of constructing a database of monthly

683 climate observations and associated high-resolution grids, Int. J. Climatol., 25, 693-712,
684 2005.

685 Mueller, B., Hirschi, M., Jimenez, C., Ciais, P., Dirmeyer, P. A., Dolman, A. J., Fisher, J. B.,
686 Jung, M., Ludwig, F., Maignan, F., Miralles, D., McCabe, M. F., Reichstein, M.,
687 Sheffield, J., Wang, K. C., Wood, E. F., Zhang, Y., and Seneviratne, S. I.: Benchmark
688 products for land evapotranspiration: LandFlux-EVAL multi-dataset synthesis, Hydrol.
689 Earth Syst. Sci., 17, 3707-3720, doi:10.5194/hess-17-3707-2013, 2013.

690 Muller, J.-P., López, G., Watson, G., Shane, N., Kennedy, T., Yuen, P., Lewis, P., Fischer, J.,
691 Guanter, L., Doménech, C., Preusker, R., North, P., Heckel, A., Danne, O., Krämer, U.,
692 Zühlke, M., Brockmann, C., and Pinnock, S.: The ESA GlobAlbedo Project for mapping
693 the Earth's land surface albedo for 15 Years from European Sensors., paper presented at
694 IEEE Geoscience and Remote Sensing Symposium (IGARSS) 2012, IEEE, Munich,
695 Germany, 22-27.7.12, 2012.

696 | [Orth, R., and Seneviratne, S.I.: Analysis of soil moisture memory from observations in](#)
697 [Europe. J. Geophys. Res. - Atmospheres, 117, D15115, 2012.](#)

698 | Pielke, R.A., Avissar, R., Raupach, M., Dolman, A.J., Zeng, X.B., and Denning, A.S.:
699 | Interactions between the atmosphere and terrestrial ecosystems: influence on weather and
700 | climate, Glob. Chang. Biol. 4 (5), 461–475, 1998.

701 | [Ping, C.L., Michaelson, G.J., Jorgenson, M.T., Kimble, J.M., Epstein, H., Romanovsky,](#)
702 [V.E., and Walker, D.A.: High stocks of soil organic carbon in the North American Arctic](#)
703 [region, Nat. Geosci., 1, 615-619, 2008.](#)

704 | [Porada, P., Ekici, A., and Beer, C.: Effects of bryophyte and lichen cover on permafrost soil](#)
705 [temperature at large scale, The Cryosphere Discuss., doi:10.5194/tc-2015-223, in review,](#)
706 [2016.](#)

707 Raddatz, T. J., Reick, C., Knorr, W., Kattge, J., Roeckner, E., Schnur, R., Schnitzler, K.-G.,
708 Wetzel, P., and Jungclaus, J. H.: Will the tropical land biosphere dominate the climate-
709 carbon cycle feedback during the twenty-first century?, Climate Dyn., doi:
710 10.1007/s00382-007-0247-8, 2007.

711 Rienecker, M. M., Suarez, M. J., Gelaro, R., Todling, R., Bacmeister, J., Liu, E., Bosilovich,
712 M. G., Schubert, S. D., Takacs, L., Kim, G.-K., Bloom, S., Chen, J., Collins, D., Conaty,
713 A., da Silva, A., Gu, W., Joiner, J., Koster, R. D., Lucchesi, R., Molod, A., Owens, T.,
714 Pawson, S., Pegion, P., Redder, C. R., Reichle, R., Robertson, F. R., Ruddick, A. G.,
715 Sienkiewicz, M., and Woollen, J: MERRA - NASA's Modern-Era Retrospective Analysis
716 for Research and Applications, J. Climate, 24, 3624-3648, doi:10.1175/JCLI-D-11-
717 00015.1, 2011.

718 Rudolf, B., and Rubel, F.: Global precipitation, In: Hantel. M. (ed): Observed global climate,
719 Chap. 11. Landolt–Boernstein: numerical data and functional relationships in science and
720 technology – new series, Group 5: Geophysics, vol. 6, Springer, Berlin Heidelberg New
721 York, p 567, 2005.

722 Schuur, E. A. G., Bockheim, J., Canadell, J. G., Euskirchen, E., Field, C. B., Goryachkin, S.
723 V., Hagemann, S., Kuhry, P., Lafleur, P. M., Lee, H., Mazhitova, G., Nelson, F. E.,
724 Rinke, A., Romanovsky, V. E., Shiklomanov, N., Tarnocai, C., Venevsky, S., Vogel, J.
725 G., and Zimov, S. A.: Vulnerability of permafrost carbon to climate change: Implications
726 for the global carbon cycle, Bioscience, 58, 701–714, doi:10.1641/B580807, 2008.

727 Seneviratne, S. I., and Stöckli, R.: The role of land-atmosphere interactions for climate
728 variability in Europe, In: Climate Variability and Extremes during the Past 100 years,
729 Brönnimann et al. (eds.), Adv. Global. Change. Res., 33, Springer Verlag. (Book chapter),
730 2008.

- 731 Seneviratne, S. I., Lüthi, D., Litschi, M., and Schär, C.: Land-atmosphere coupling and
732 climate change in Europe, *Nature*, 443, 205-209, 2006.
- 733 Seneviratne, S. I., Corti, T., Davin, E., Hirschi, M., Jaeger, E. B., Lehner, I., Orlowsky, B.,
734 and Teuling, A. J.: Investigating soil moisture-climate interactions in a changing climate:
735 A review, *Earth-Sci. Rev.*, 99, 125-161, doi:10.1016/j.earscirev.2010.02.004, 2010.
- 736 Serreze, M. C., and Barry, R. G.: Processes and impacts of Arctic amplification: A research
737 synthesis, *Global Planet Change*, 77, 85-96, doi:10.1016/j.gloplacha.2011.03.004, 2011.
- 738 Slater, A., Pitman, A., and Desborough, C.: Simulation of freeze thaw cycles in a general
739 circulation model land surface scheme, *J. Geophys. Res.*, 103, 11303–1131, 1998.
- 740 Solomon, S., Qin, D., Manning, M., Marquis, M., Averyt, K., Tignor, M. M. B., Miller Jr., H.
741 L., and Chen, Z. (Eds.): *Climate change 2007: The physical science basis*, Cambridge
742 University Press, 996 pp., 2007.
- 743 Stacke, T., and Hagemann, S.: Development and validation of a global dynamical wetlands
744 extent scheme, *Hydrol. Earth Syst. Sci.*, 16, 2915-2933, doi:10.5194/hess-16-2915-2012,
745 2012.
- 746 Stevens, B., Giorgetta, M., Esch, M., Mauritsen, T., Crueger, T., Rast, S., Salzmann, M.,
747 Schmidt, H., Bader, J., Block, K., Brokopf, R., Fast, I., Kinne, S., Kornblueh, L.,
748 Lohmann, U., Pincus, R., Reichler, T., and Roeckner, E.: The atmospheric component of
749 the MPI-M Earth System Model: ECHAM6, *J. Adv. Model Earth Syst.*, 5, 146-172.
750 doi:10.1002/jame.20015, 2013.
- 751 Swenson, S. C., Lawrence, D. M., and Lee, H.: Improved simulation of the terrestrial
752 hydrological cycle in permafrost regions by the Community Land Model, *J. Adv. in
753 Modelling Earth Systems*, 4, doi:10.1029/2012MS000165, 2012.
- 754 Takala, M., Luojus, K., Pulliainen, J., Derksen, C., Lemmetyinen, J., Kärnä, J.-P., Koskinen,

- 755 J., and Bojkov, B.: Estimating northern hemisphere snow water equivalent for climate
756 research through assimilation of spaceborne radiometer data and ground-based
757 measurements, *Rem. Sens. Environ.*, 115, doi: 10.1016/j.rse.2011.08.014, 2011.
- 758 [Takata, K., and Kimoto, M.: A numerical study on the impact of soil freezing on the](#)
759 [continental-scale seasonal cycle, J. Meteor. Soc. Japan, 78, 199-221, 2000.](#)
- 760 [Tarnocai, C., Canadell, J. G., Schuur, E. A. G., Kuhry, P., Mazhitova, G., and Zimov, S.: Soil](#)
761 [organic carbon pools in the northern circumpolar permafrost region, Global Biogeochem](#)
762 [Cycles, 23, doi:10.1029/2008GB003327, 2009.](#)
- 763 Taylor, C. M., Birch, C. E., Parker, D. J., Dixon, N., Guichard, F., Nikulin, G., and Lister, G.
764 M. S.: Modeling soil moisture-precipitation feedback in the Sahel: Importance of spatial
765 scale versus convective parameterization, *Geophys. Res. Lett.*, 40, 6213–6218,
766 doi:10.1002/2013GL058511, 2013.
- 767 Taylor, K. E., Williamson, D., and Zwiers, F.: The sea surface temperature and sea-ice
768 concentration boundary conditions for AMIP II simulations, PCMDI Report, 60, Program
769 for Climate Model Diagnosis and Intercomparison. Lawrence Livermore National
770 Laboratory, Livermore, California, 25 pp., 2000.
- 771 Taylor, K. E., Stouffer, R. J., and Meehl, G. A.: An overview of CMIP5 and the experiment
772 design, *Bull. Amer. Meteor. Soc.*, 93 (4), 485-498, 2012.
- 773 Teuling, A. J., Hirschi, M., Ohmura, A., Wild, M., Reichstein, M., Ciais, P., Buchmann, N.,
774 Ammann, C., Montagnani, L., Richardson, A. D., Wohlfahrt, G., and Seneviratne, S. I.: A
775 regional perspective on trends in continental evaporation, *Geophys. Res. Lett.*, 36,
776 L02404, doi:10.1029/2008GL036584, 2009.
- 777 Walsh, J. E., Anisimov, O., Hagen, J. O. M., Jakobsson, T., Oerlemans, J., Prowse, T. D.,
778 Romanovsky, V., Savelieva, N., Serreze, M., Shiklomanov, A., Shiklomanov, I.,

779 Solomon, S., Arendt, A., Atkinson, D., Demuth, M. N., Dowdeswell, J., Dyurgerov, M.,
780 Glazovsky, A., Koerner, R. M., Meier, M., Reeh, N., Sigurosson, O., Steffen, K., and
781 Truffer, M.: Cryosphere and hydrology, in: Symon C, Arris L, Heal B (eds.) Arctic
782 Climate Impact Assessment, Chap. 6: 184-242, Cambridge University Press, 2005.

783 Weedon, G. P., Balsamo, G., Bellouin, N., Gomes, S., Best, M. J., and Viterbo, P.: The
784 WFDEI meteorological forcing data set: WATCH Forcing Data methodology applied to
785 ERA-Interim reanalysis data, Water Resour. Res., 50, doi:10.1002/2014WR015638,
786 2014.

787 | [Zimov, S. A., Davydov, S. P., Zimova, G. M., Davydova, A. I., Schuur, E. A. G., Dutta, K.,](#)
788 | [and Chapin III, F. S.: Permafrost carbon: Stock and decomposability of a globally](#)
789 | [significant carbon pool, Geophys Res. Lett., 33, doi:10.1029/2006GL027484, 2006.](#)

790

791 **Figure captions**

792 **Fig. 1** Distribution of permafrost areas in the Arctic according to a) Brown et al. (1997), b)
793 ECH6-REF, and c) ECH6-PF.

794 **Fig. 1** Boreal summer (JJA) precipitation differences [%] relative to WFDEI data for a)
795 ECH6-REF, b) ECH6-PF, and c) difference between ECH6-PF and ECH6-REF [in
796 % of WFDEI precipitation].

797 **Fig. 2****Fig. 3** Boreal summer (JJA) 2m temperature differences [K] to WFDEI data for a)
798 ECH6-REF, b) ECH6-PF, and c) difference between ECH6-PF and ECH6-REF.

799 **Fig. 3****Fig. 4** Boreal summer (JJA) surface solar incoming radiation differences [W/m²] to
800 CERES data for a) ECH6-REF, b) ECH6-PF, and c) difference between ECH6-PF
801 and ECH6-REF.

802 **Fig. 4****Fig. 5** Catchments of the Baltic Sea and of the six largest Arctic rivers (from left to
803 right: Mackenzie, Baltic Sea, Northern Dvina, Ob, Yenisei, Lena, Kolyma).

804 **Fig. 5****Fig. 6** Mean monthly climatology (1989-2009) of discharge (upper panels) and
805 precipitation (lower panels) over the 6 largest Arctic river catchments (left column)
806 and the Baltic Sea catchment (land only, right column). Observations comprise
807 climatological observed discharge and WFDEI precipitation, respectively.

808 **Fig. 6****Fig. 7** Mean monthly climatology (1989-2009) of evapotranspiration (upper panels)
809 and relative root zone soil moisture (lower panels) over the 6 largest Arctic river
810 catchments (left column) and the Baltic Sea catchment (land only, right column).
811 Evapotranspiration data comprise the mean, minimum and maximum diagnostic
812 estimates from the LandFlux Eval (LF) dataset. The dashed blue line (PF-Total)
813 denotes the total root zone moisture content (liquid + frozen) for ECH6-PF.

814 **Fig. 7****Fig. 8** Mean frozen fraction of total root zone soil moisture (1989-2009) in ECH6-PF
815 over the 6 largest Arctic river catchments (solid curve) and the Baltic Sea catchment

816 | [\(land only, dashed curve\)](#)

817 | [Fig. 8](#)[Fig. 9](#) Mean monthly climatological differences (1989-2009) of between ECH6-PF
818 | and ECH6-REF for precipitation (ΔP) and evapotranspiration (ΔET) over the 6
819 | largest Arctic rivers (upper panel) and the Baltic Sea catchment (lower panel). The
820 | dashed lines indicate the corresponding spreads obtained from MPI-ESM simulations
821 | of deVrese et al. (2016).

822 | [Fig. 9](#)[Fig. 10](#) Mean monthly climatology (1989-2009) of 2m temperature differences to
823 | WFDEI data (upper panels) and surface solar irradiance (SSI; lower panels) over the
824 | 6 largest Arctic river catchments (left column) and the Baltic Sea catchment (land
825 | only, right column). SSI observations comprise CERES data for 2000-2010.

826 | [Fig. 10](#)[Fig. 11](#) Mean monthly climatology (1989-2009) of surface albedo (upper panels) and
827 | snow pack snow water equivalent (SWE; lower panels) over the 6 largest Arctic river
828 | catchments (left column) and the Baltic Sea catchment (land only, right column).
829 | Albedo observations data from MODIS (2000-2011), CERES (2000-2010) and
830 | GlobAlbedo (1998-2011), SWE observations comprise data from GlobSnow (1989-
831 | 2009), MERRA (1979-2013), and SDC climatology.

832 | [Fig. 11](#)[Fig. 12](#) Chain of processes involved in the soil moisture precipitation feedback over
833 | high latitudes. Red arrows indicate the initiation of the positive feedback loop by the
834 | presence of frozen soil,, blue arrows indicate the loop itself.

835 | [Fig. 12 Correlation of soil moisture and precipitation for a\) ECH6-REF, b\) ECH6-PF, and c\)](#)
836 | [difference between ECH6-PF and ECH6-REF.](#)

837 | [Fig. 13 Number of months where in the climatological average of 1989-2009, the upper soil](#)
838 | [layer is below 0°C in ECH6-PF.](#)

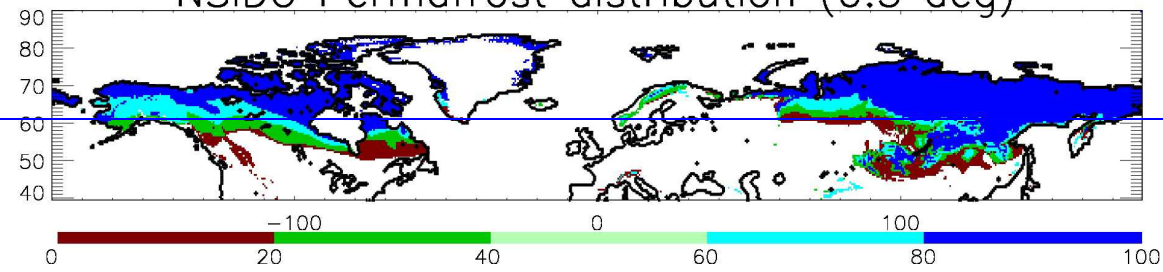
839

840

841

842

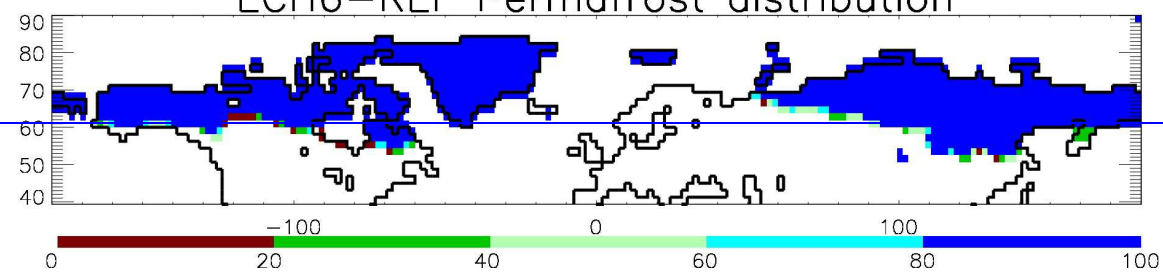
NSIDC Permafrost distribution (0.5 deg)



843

b) —

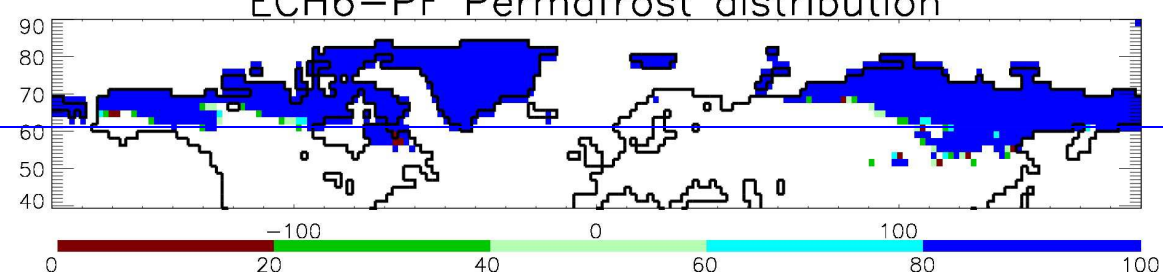
ECH6-REF Permafrost distribution



845

e) —

ECH6-PF Permafrost distribution



847

848
849 Distribution of permafrost areas in the Arctic according to a) Brown et al. (1997), b) ECH6-
850 REF, and c) ECH6-PF.

851

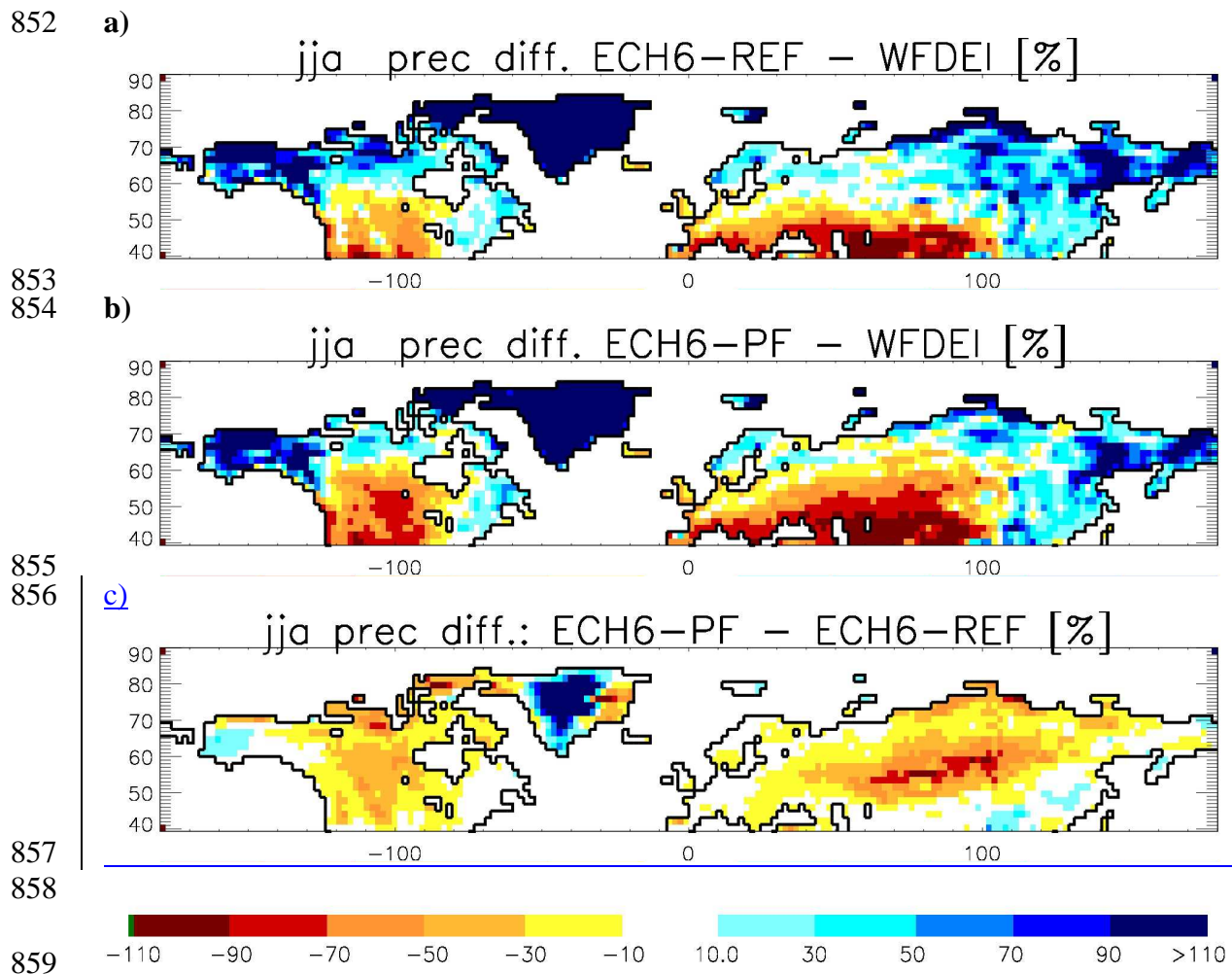
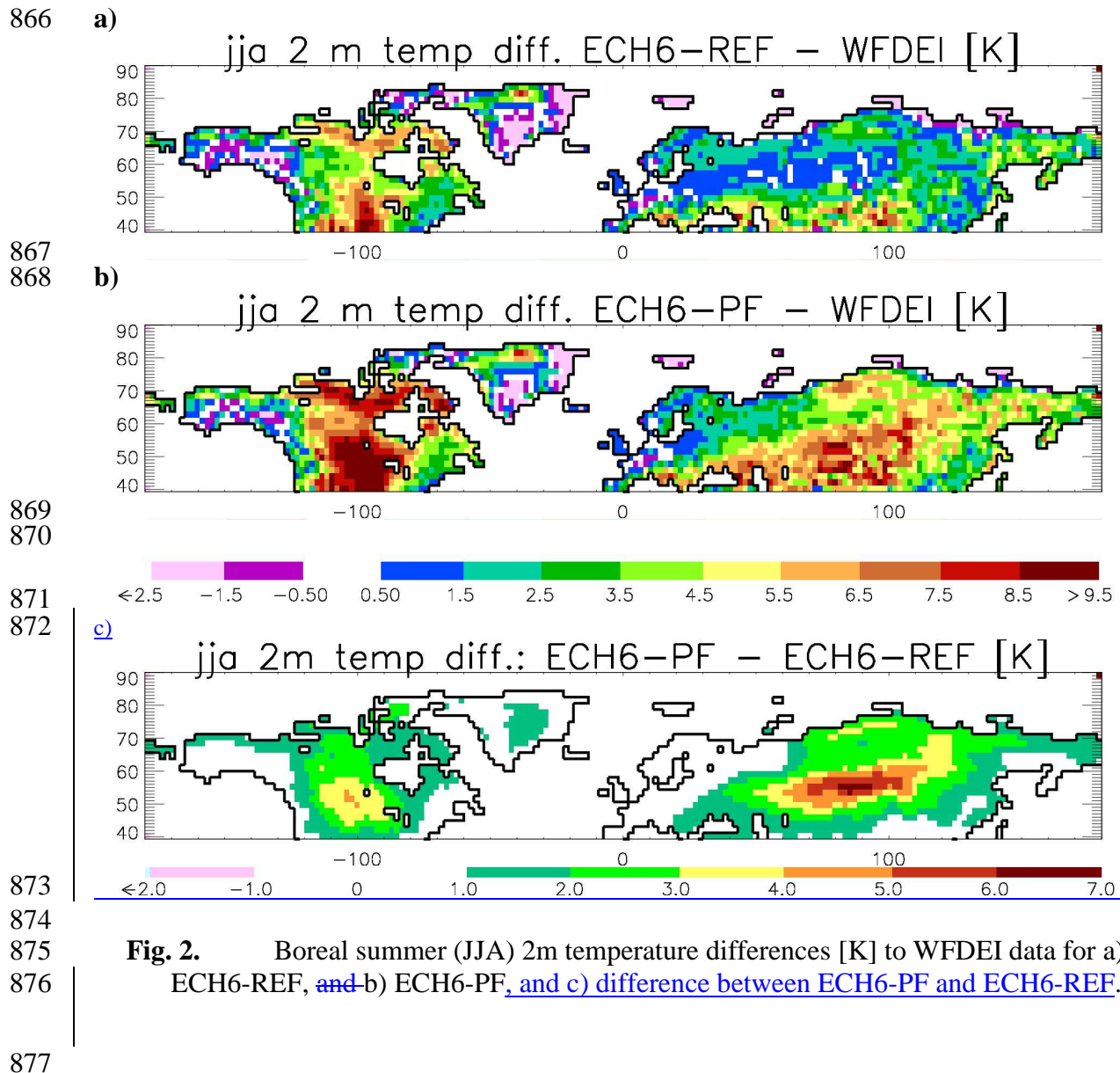


Fig. 1. Boreal summer (JJA) precipitation differences [%] relative to WFDEI data for a) ECH6-REF, and b) ECH6-PF, and c) difference between ECH6-PF and ECH6-REF [in % of WFDEI precipitation].



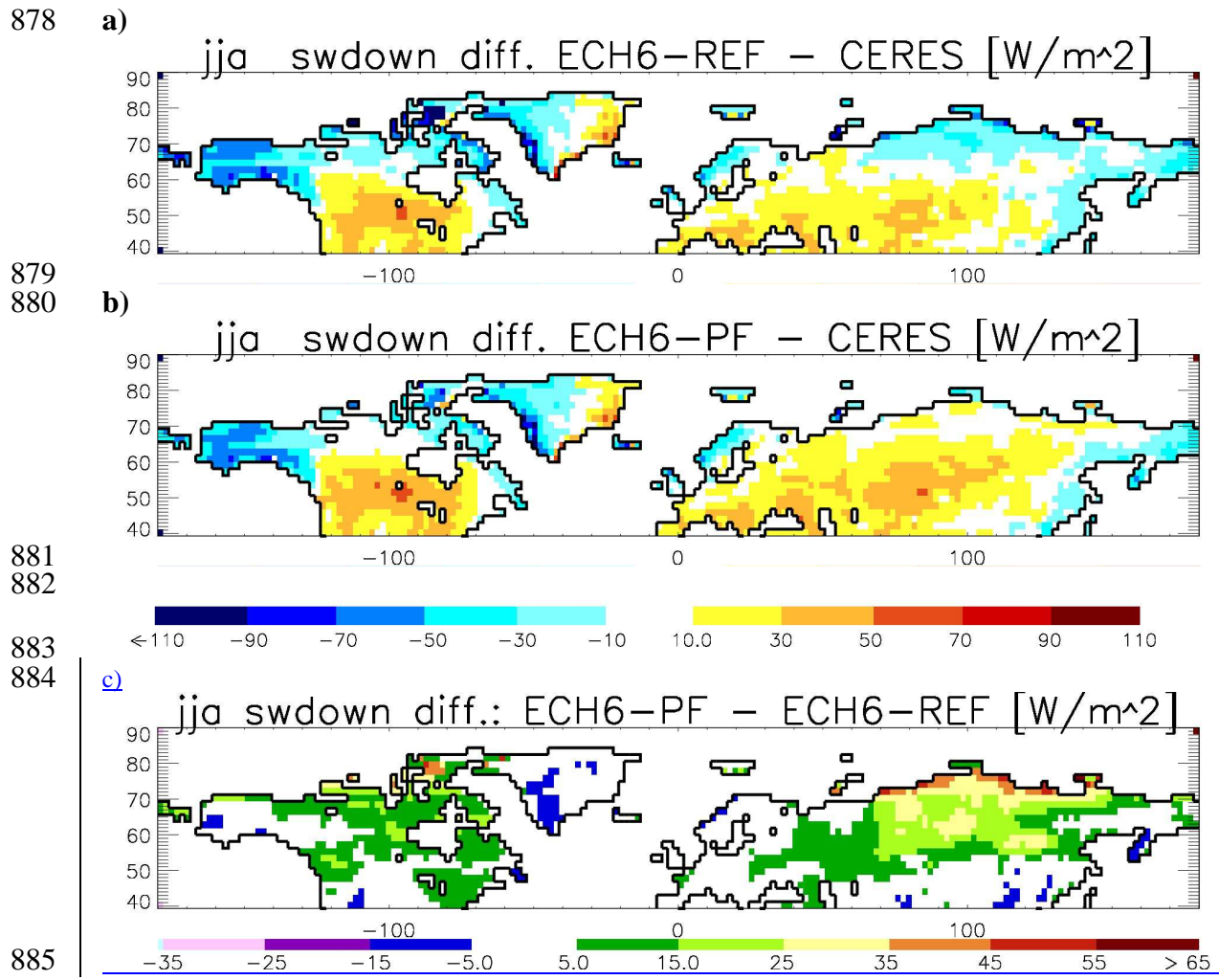
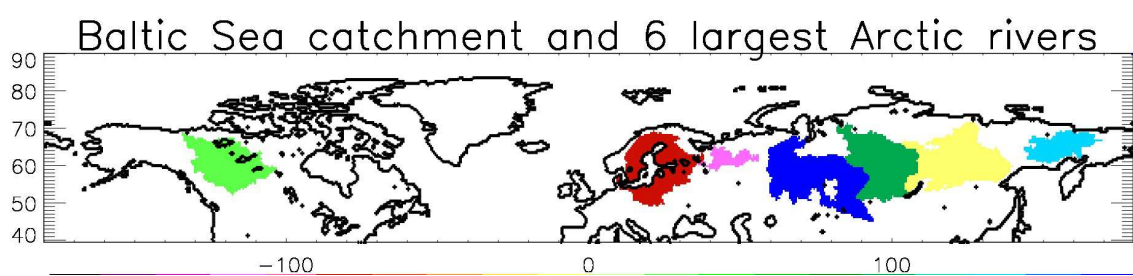


Fig. 3. Boreal summer (JJA) surface solar incoming radiation differences [W/m²] to CERES data for a) ECH6-REF, [and](#) b) ECH6-PF, [and](#) c) difference between ECH6-PF [and](#) ECH6-REF.

892
893

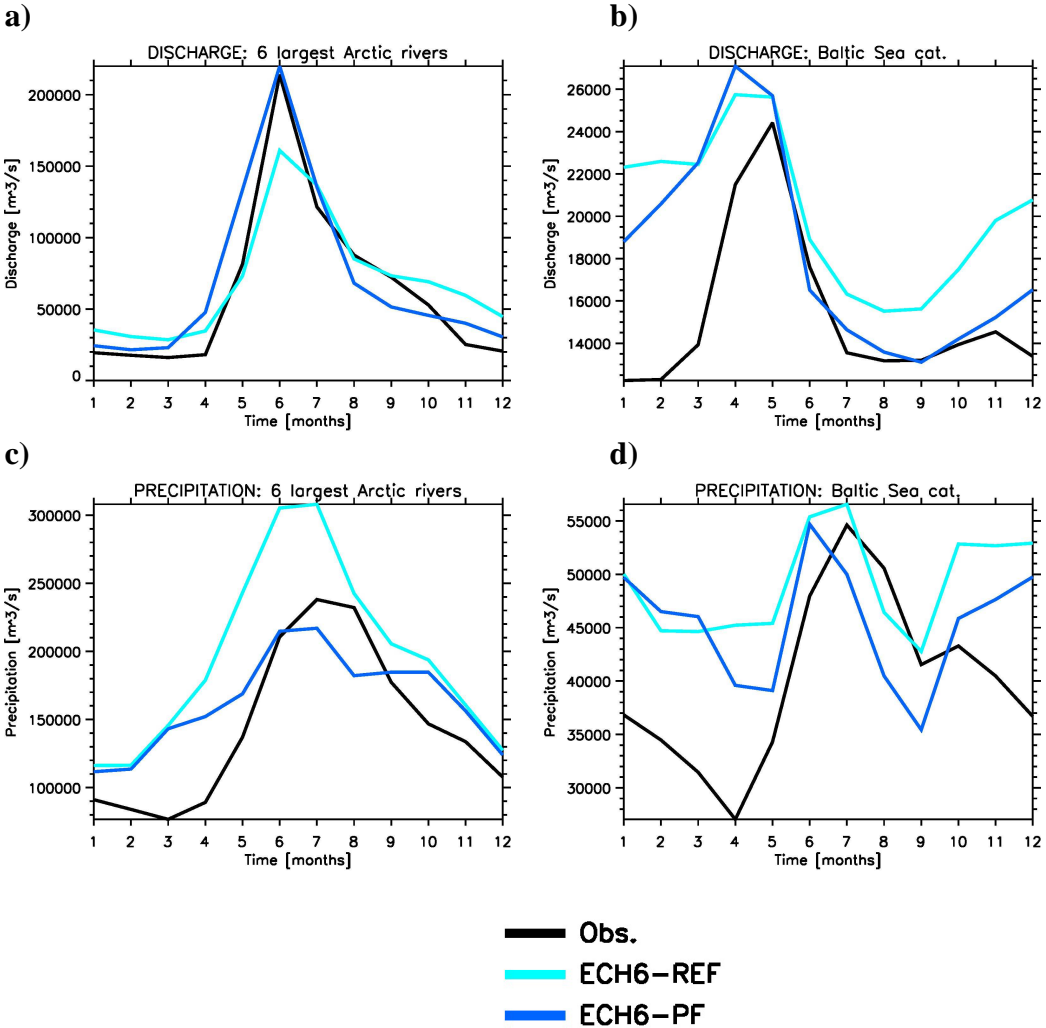


894
895
896
897
898

Fig. 4. Catchments of the Baltic Sea and of the six largest Arctic rivers (from left to right: Mackenzie, Baltic Sea, Northern Dvina, Ob, Yenisei, Lena, Kolyma).

899
900
901
902

903



904

905

906

907

908

909

910

911

912

913

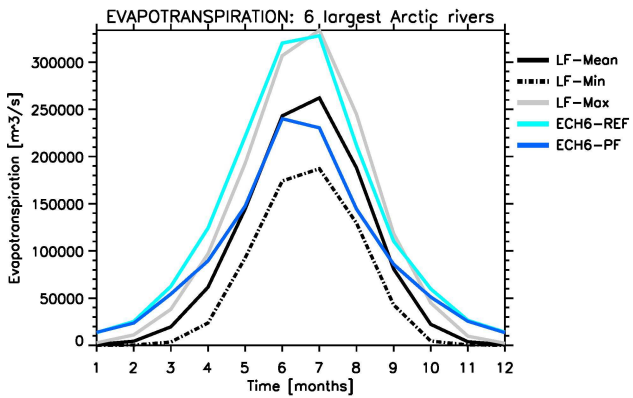
Fig. 5. Mean monthly climatology (1989-2009) of discharge (upper panels) and precipitation (lower panels) over the 6 largest Arctic river catchments (left column) and the Baltic Sea catchment (land only, right column). Observations comprise climatological observed discharge and WFDEI precipitation, respectively.

914

915

916

917 a)



b)

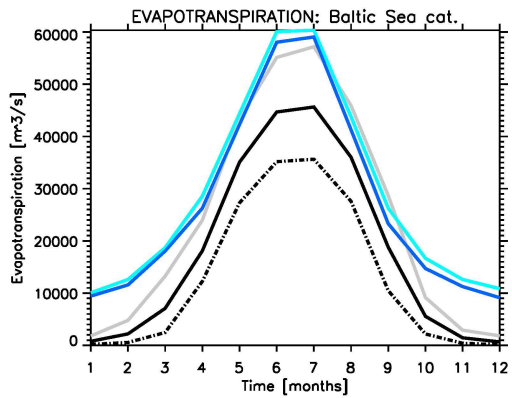
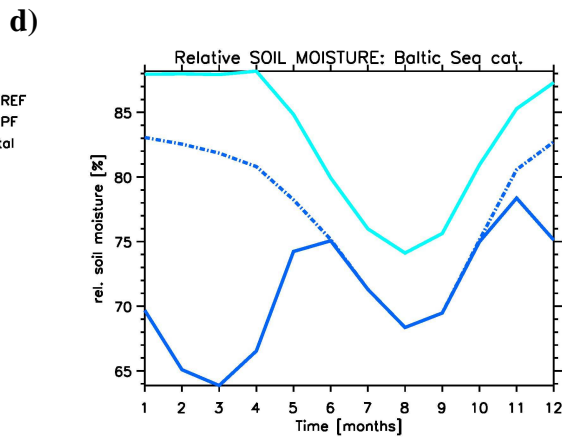
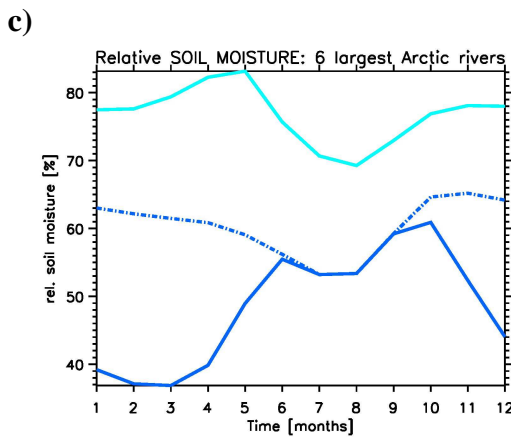
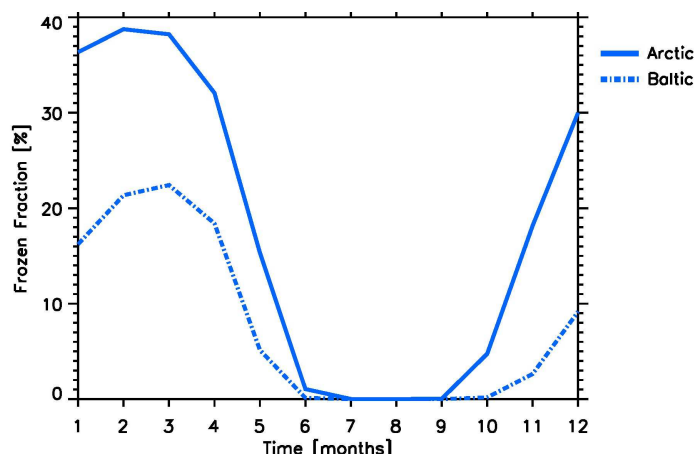
918
919920
921
922
923
924
925
926
927

Fig. 6. Mean monthly climatology (1989-2009) of evapotranspiration (upper panels) and relative root zone soil moisture (lower panels) over the 6 largest Arctic river catchments (left column) and the Baltic Sea catchment (land only, right column). Evapotranspiration data comprise the mean, minimum and maximum diagnostic estimates from the LandFlux Eval (LF) dataset. The dashed blue line ([PF-Total](#)) denotes the total root zone [water moisture](#) content (liquid + frozen) for ECH6-PF.

928
929

930



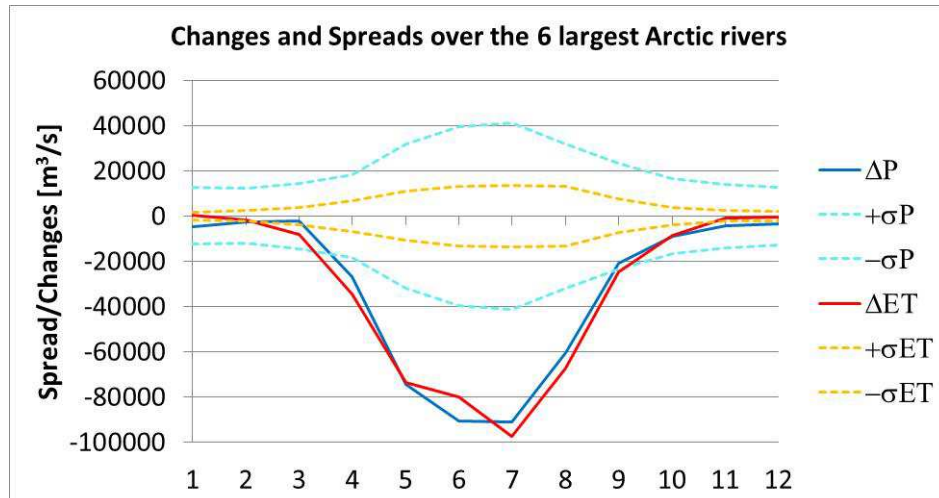
931

932 | **Fig. 7.** Mean frozen fraction of frozen_total root zone soil moisture (1989-2009) in
933 | ECH6-PF over the 6 largest Arctic river catchments (solid curve) and the Baltic Sea
934 | catchment (land only, dashed curve). Note that for ECH6-REF, this is zero as no freezing
935 | is regarded.

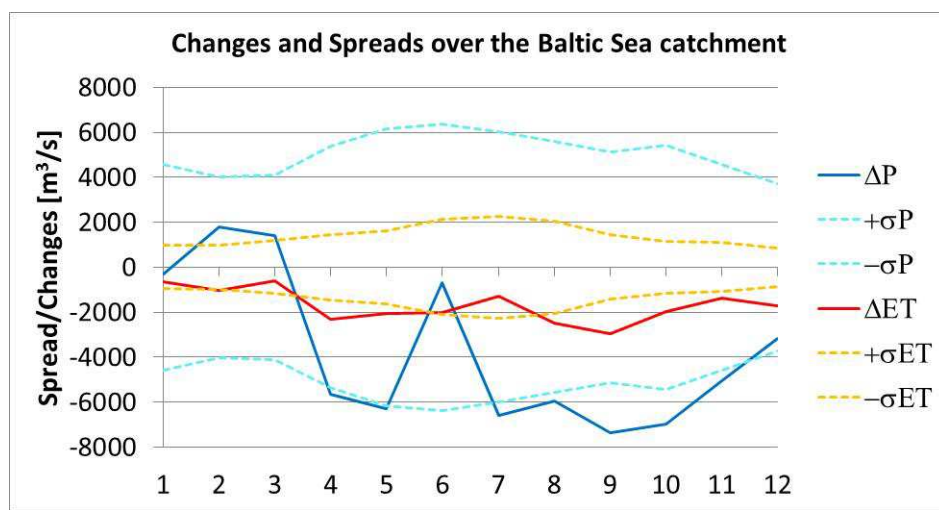
936

937

938



939



940

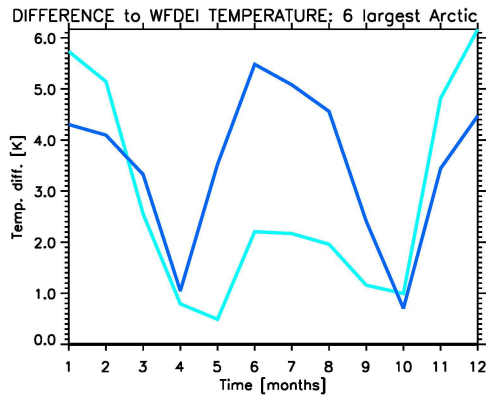
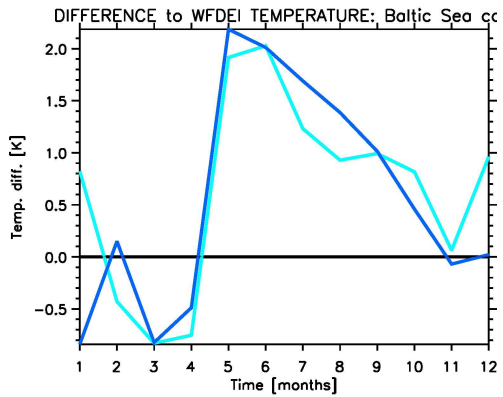
Fig. 8. Mean monthly climatological differences (1989-2009) between ECH6-PF and ECH6-REF for precipitation (ΔP) and evapotranspiration (ΔET) over the 6 largest Arctic rivers (upper panel) and the Baltic Sea catchment (lower panel). The dashed lines indicate the corresponding spreads obtained from MPI-ESM simulations of deVrese et al. (2016).

944

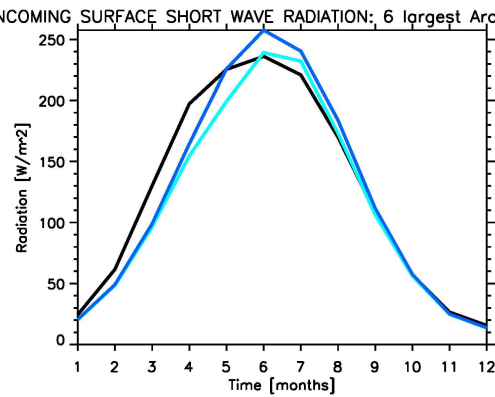
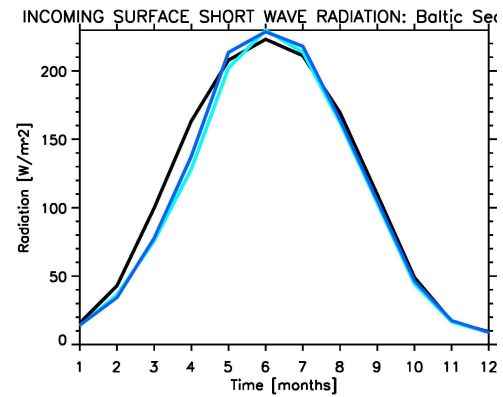
945

946

947

a)**b)**

948

c)**d)**

950

951

— Obs.
— ECH6-REF
— ECH6-PF

952

953

954

955

Fig. 9. Mean monthly climatology (1989–2009) of 2m temperature differences to WFDEI data (upper panels) and surface solar irradiance (SSI; lower panels) over the 6 largest Arctic river catchments (left column) and the Baltic Sea catchment (land only, right column). SSI observations comprise CERES data for 2000–2010.

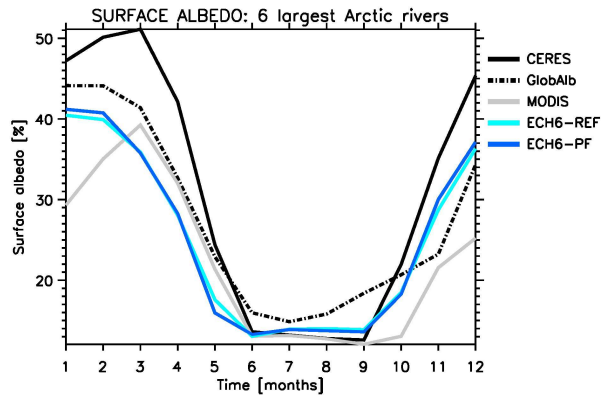
956

957

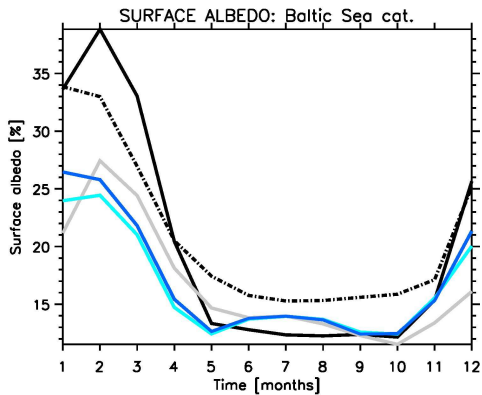
958

959

960 a)



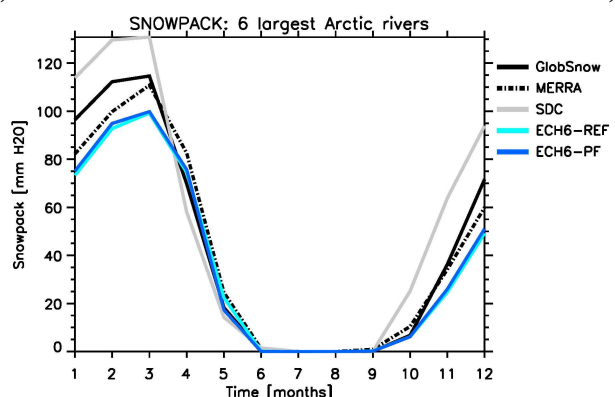
b)



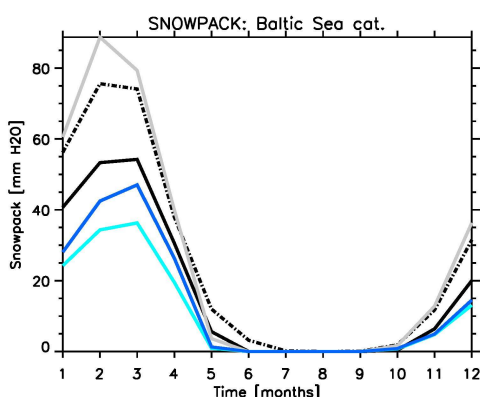
961

962

c)



d)



963

964

965

966

967

968

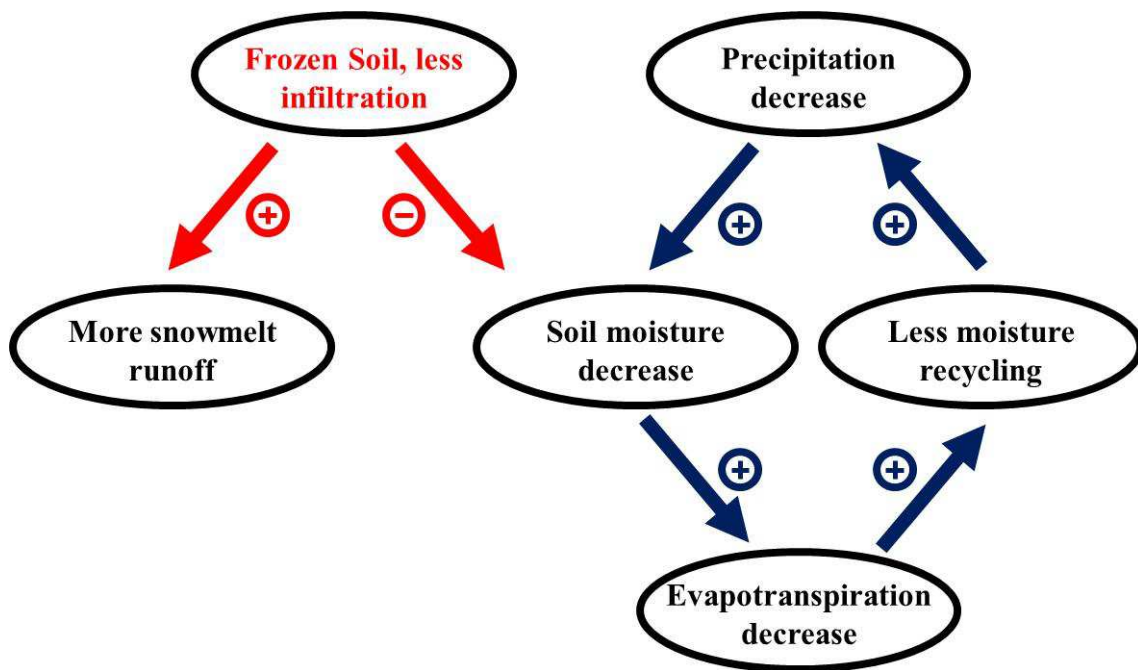
969

970

Fig. 10. Mean monthly climatology (1989-2009) of surface albedo (upper panels) and snow pack snow water equivalent (SWE; lower panels) over the 6 largest Arctic river catchments (left column) and the Baltic Sea catchment (land only, right column). Albedo observations data from MODIS (2000-2011), CERES (2000-2010) and GlobAlbedo (1998-2011), SWE observations comprise data from GlobSnow (1989-2009), MERRA (1979-2013), and SDC climatology.

971

972



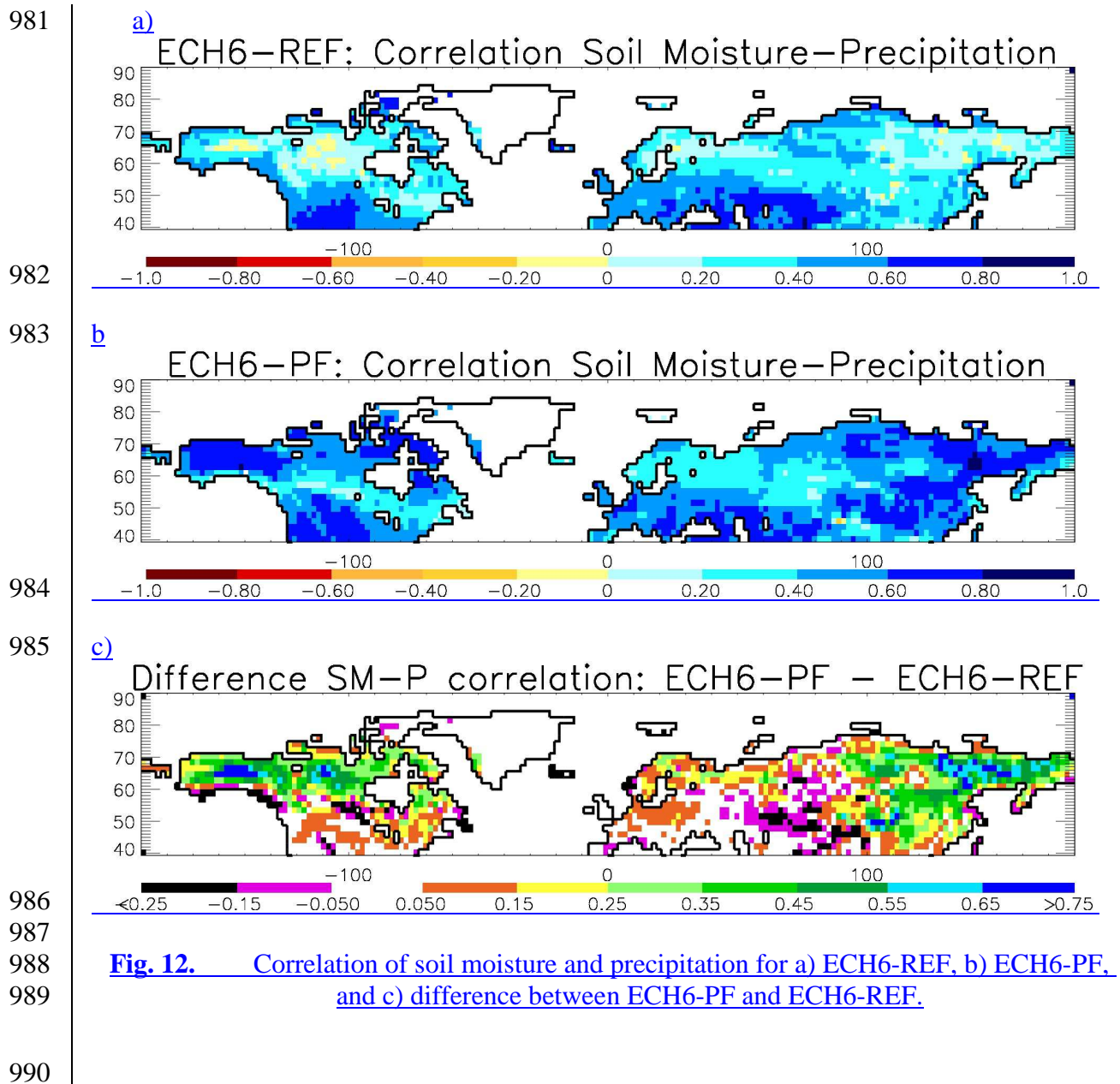
973

974

975 **Fig. 11.** Chain of processes involved in the soil moisture precipitation feedback over high
976 latitudes. Red arrows indicate the initiation of the positive feedback loop by the presence
977 of frozen soil, directions supporting this feedback, blue arrows indicate the loop
978 itself compensating opposite effects.

979

980 |



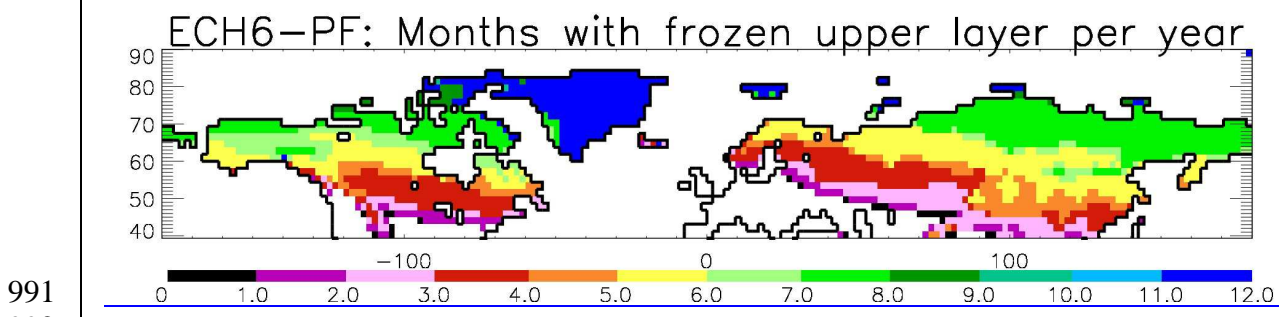


Fig. 13. Number of months where in the climatological average of 1989-2009, the upper soil layer is below 0°C in ECH6-PF.

997 **Table 1.** Summer (JJA) biases over the six largest Arctic rivers for 2m temperature (T_{2m} , to
 998 WFDEI), radiative flux (R) into the surface due to biases in SSI (to CERES), albedo (α , to
 999 GlobAlbedo) and their combined effect (comb.) as well as the estimated related impact on
 1000 surface temperature (T_s) and the contribution of the SSI bias to this impact.

Experiment	ΔT_{2m}	ΔR SSI	$\Delta R \alpha$	ΔR comb.	ΔT_s comb.	SSI cont.
ECH6-REF	2.1 K	5.0 W/m ²	4.1 W/m ²	9.0 W/m ²	1.7 K	55%
ECH6-PF	5.0 K	15.8 W/m ²	4.3 W/m ²	19.8 W/m ²	3.6 K	78%

1001

1002